Poster Talks

The preview session by the poster presenters today

#1

GRHydro simulation of BNS

Chia-Hui Lin

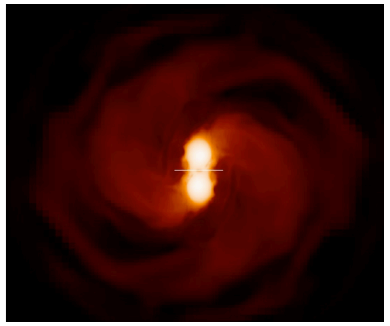

Binary neutron star merger

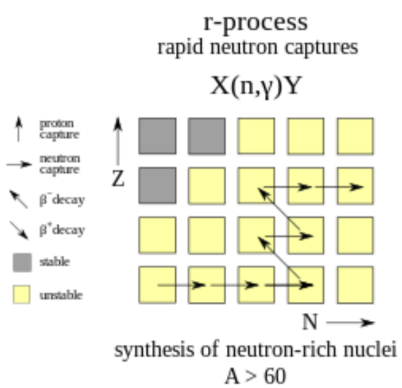

R-process
(rapid neutron-capture process)

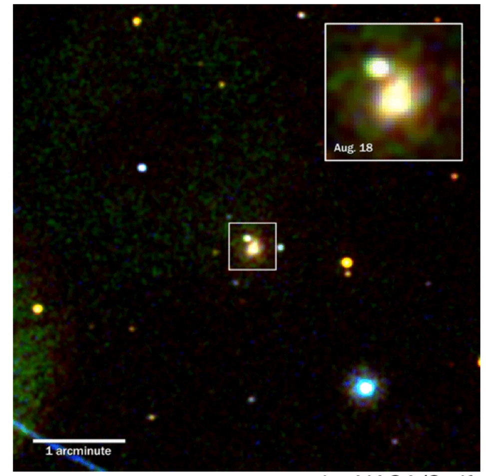

by NASA/Swift

Kilonova

- 3D GRHydro simulation with the Einstein Toolkit
- 1.44 Ms v.s. 1.44 Ms NS
- gamma law EoS
- comparison different initial background density

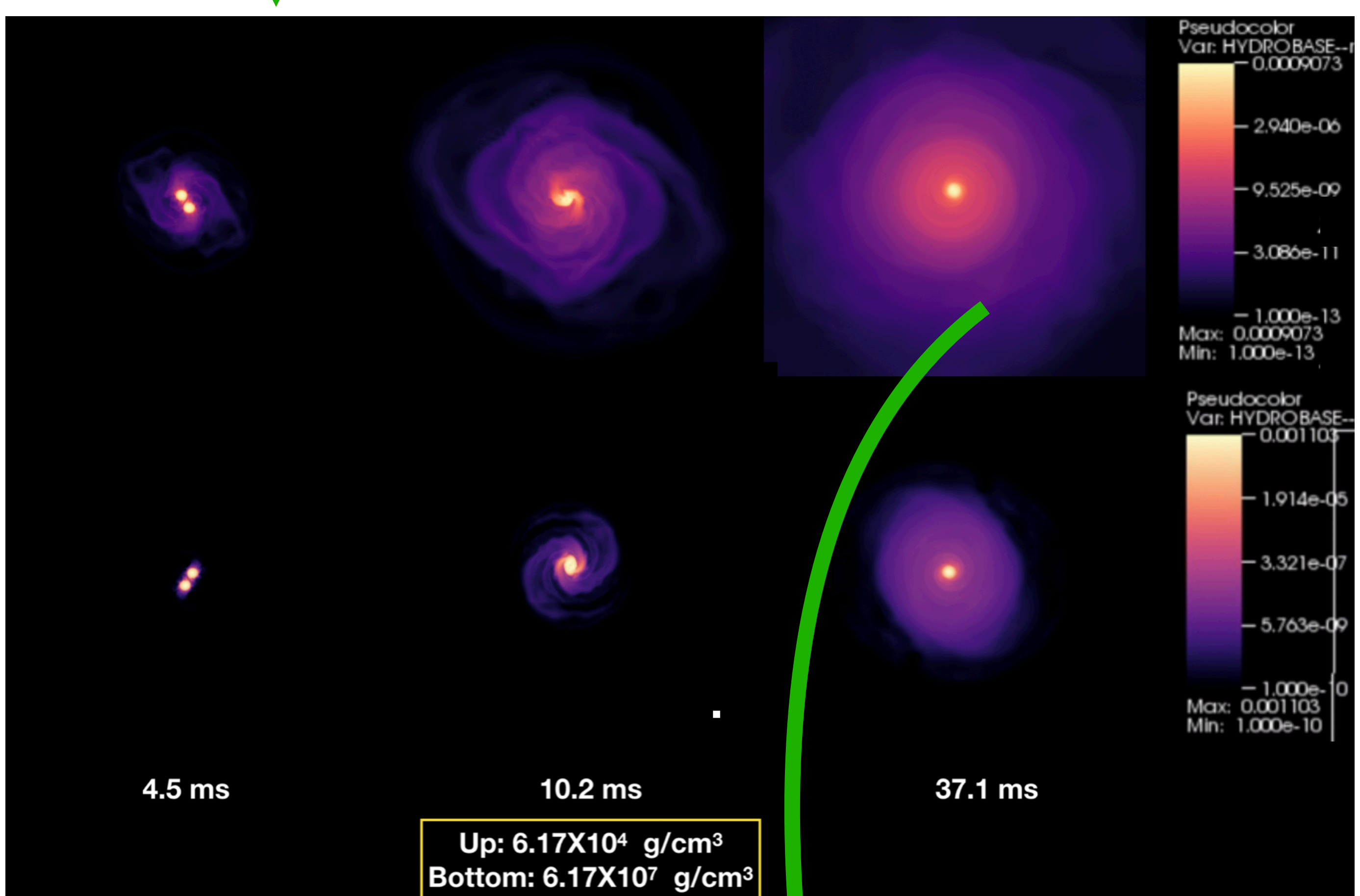

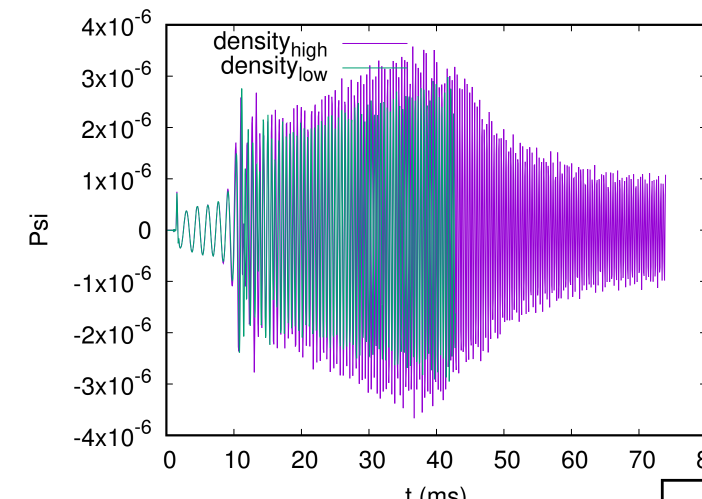

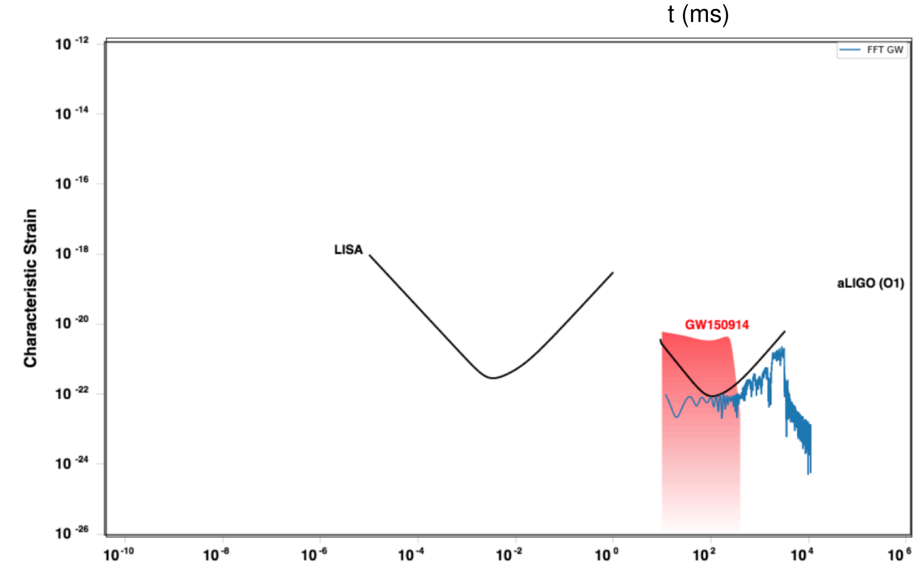

Our simulation
peak=1.82×10^{-21}
at frequency=2640.61 Hz
distance=5 Mpc

GW150914
peak~10^{-20}
at frequency~150 Hz
distance~410 Mpc

GW170817
peak~7×10^{-20}
at frequency~500 Hz
distance~40 Mpc

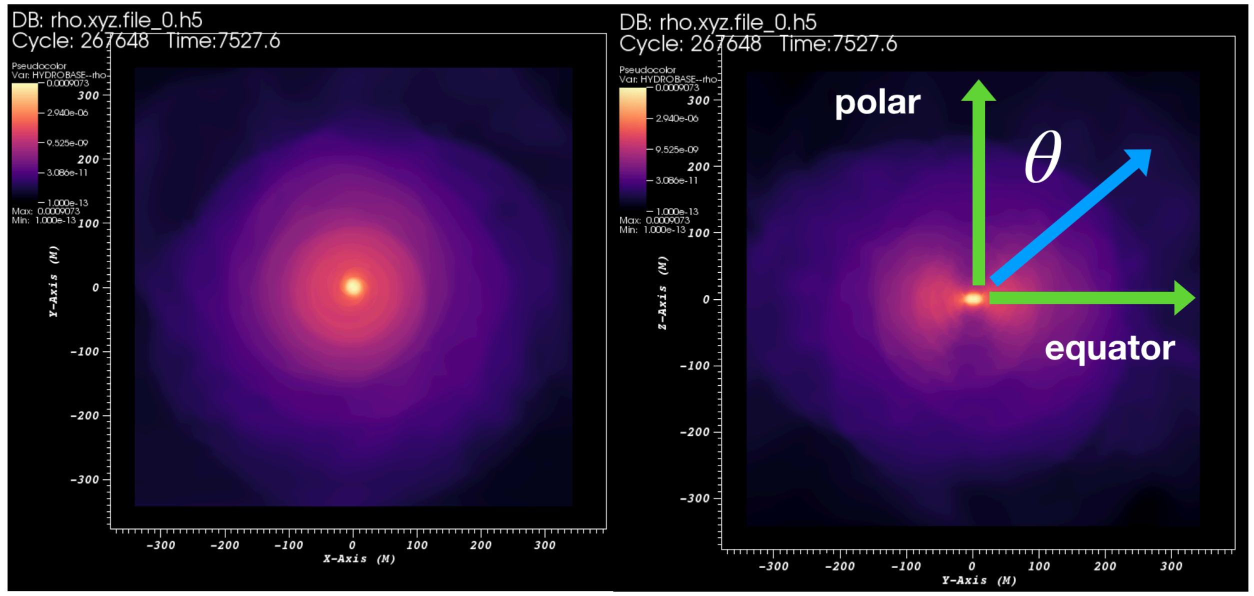

XY-plane

YZ-plane

Size:(1000 km)^2
T= 37.2 ms

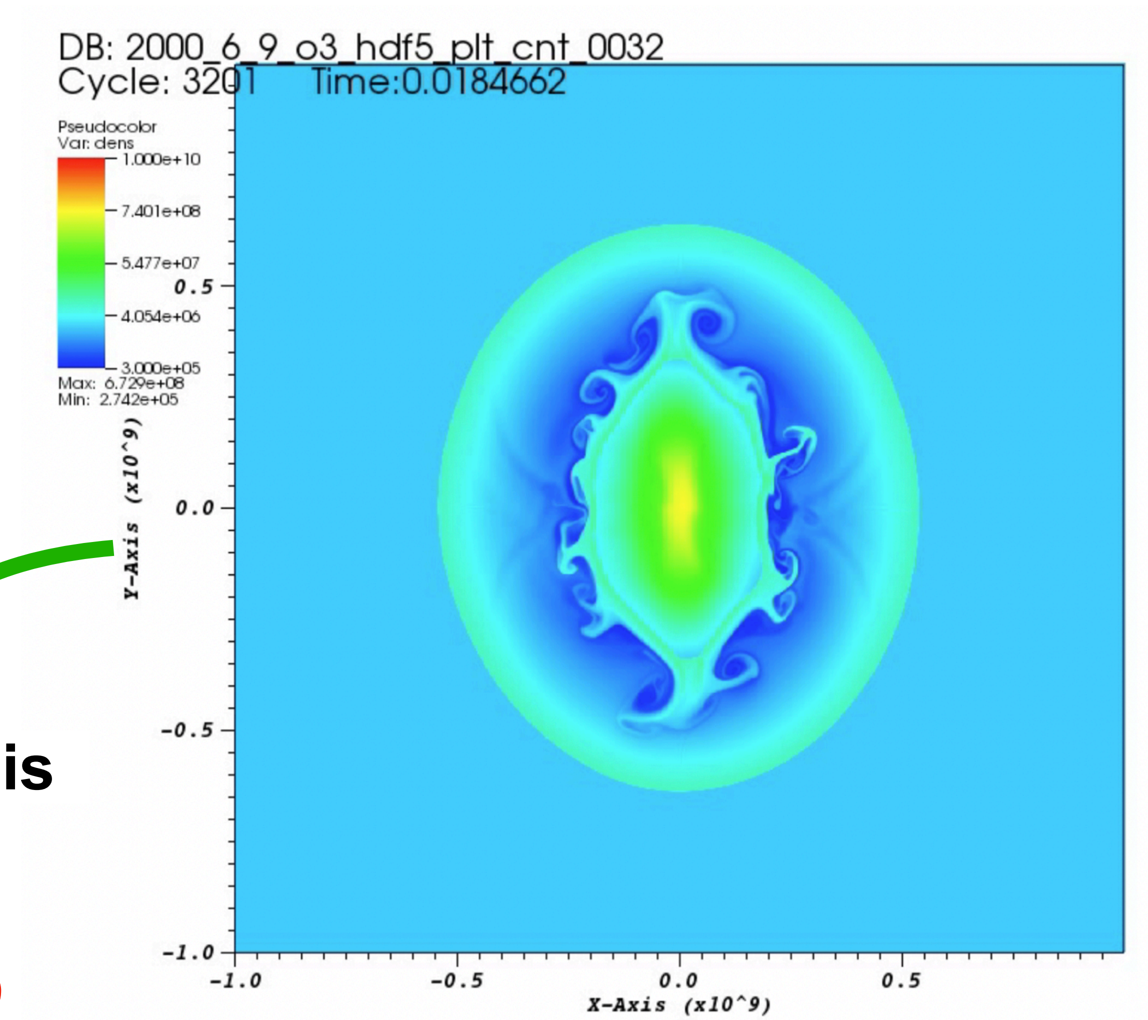

- Enlargement by FLASH code
- 2D hydrodynamic simulation
- gamma law EOS
- Self-gravity

nucleosynthesis

?

#2

Estimation of the frequency of ringdown gravitational wave using neural network

Takahiro S. Yamamoto, Takahiro Tanaka (Kyoto Univ.)

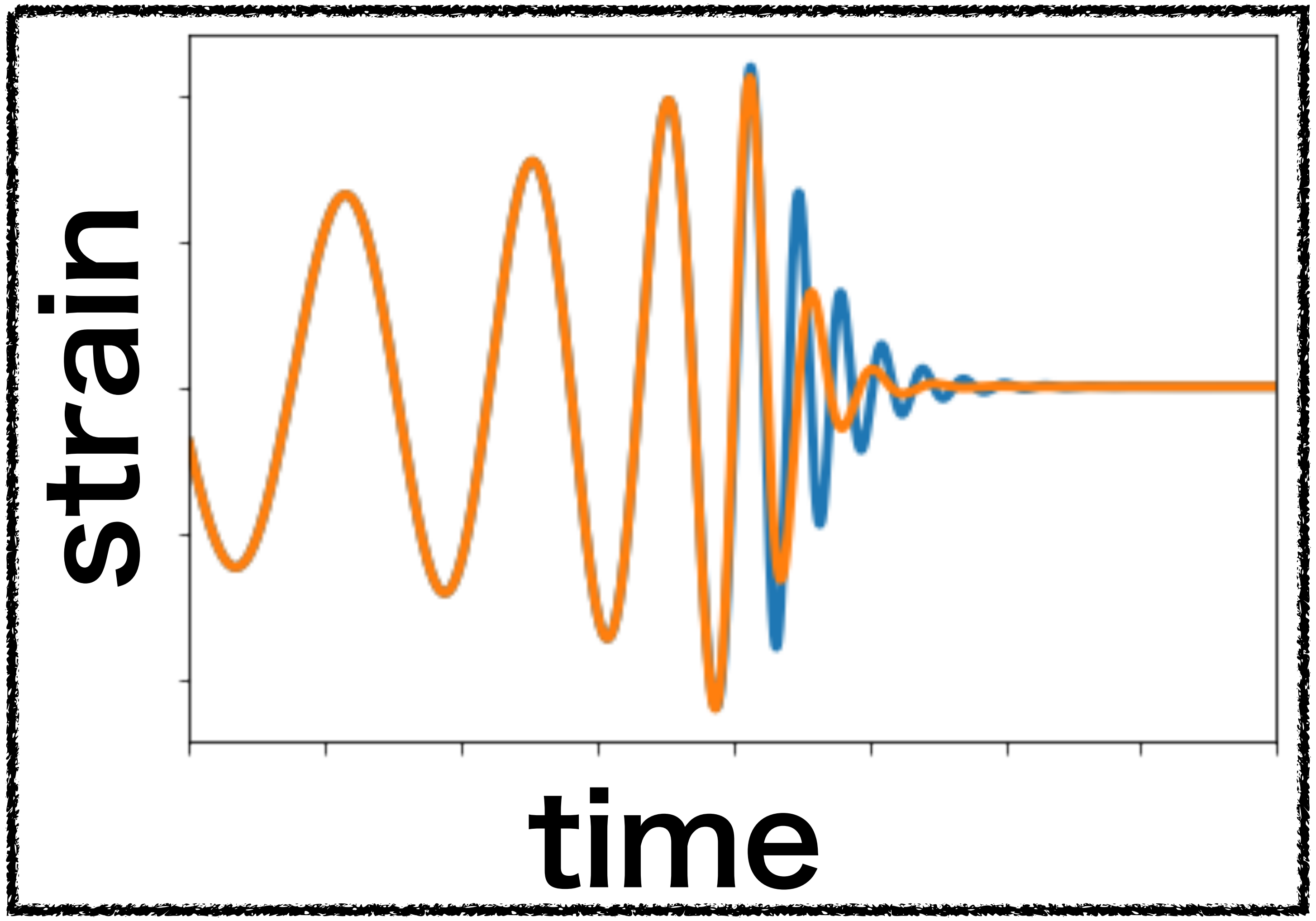

Can neural network test the GR using ringdown gravitational wave?

Estimation of the frequency of ringdown gravitational wave using neural network

Takahiro S. Yamamoto, Takahiro Tanaka (Kyoto Univ.)

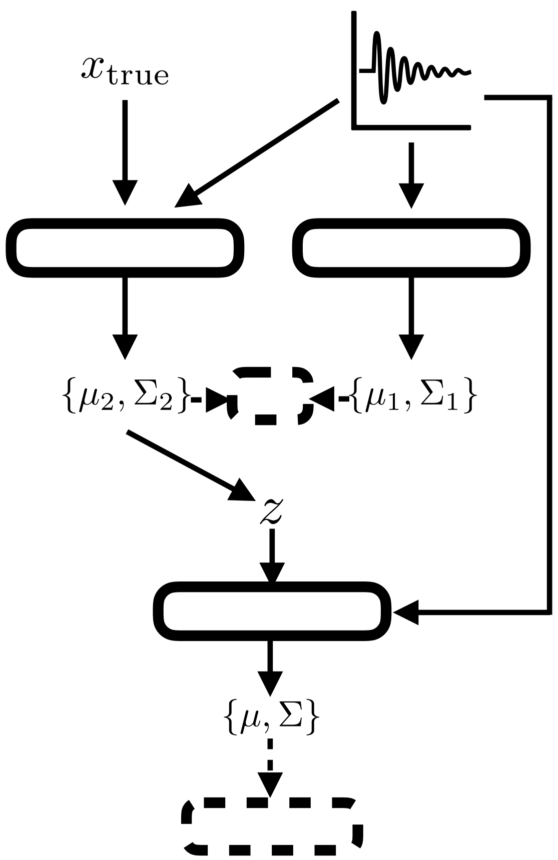

For the consistency test of GR,

NN should estimate the posterior distribution (not the point est.)

- > Bayesian inference with Conditional Variational Auto Encoder

Gabbard et al. arXiv: 1909.06296

The posterior distribution being estimated by neural network is consistent with frequentist interpretation.

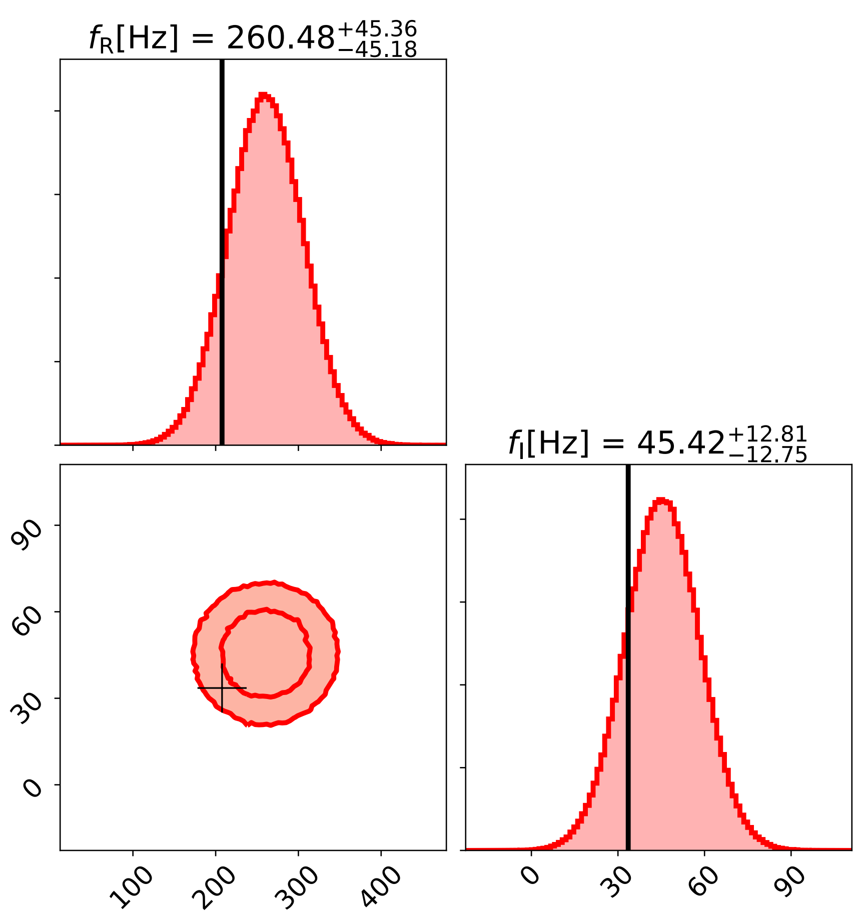

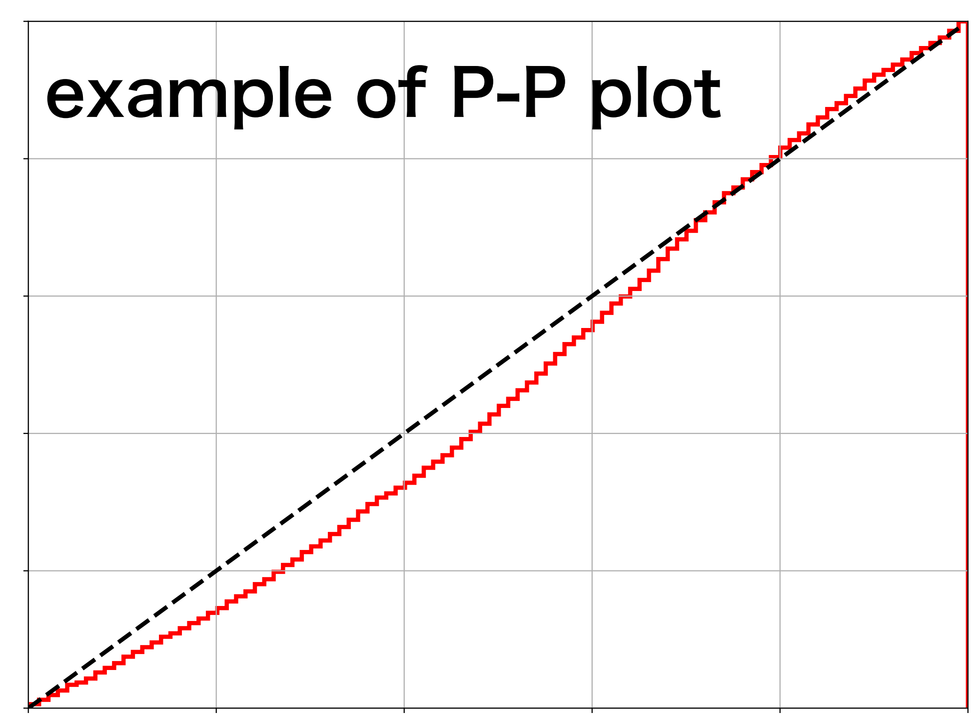

#3

Accurate Sky Localization with PE

Parameter Estimation (PE) provides accurate sky localization.

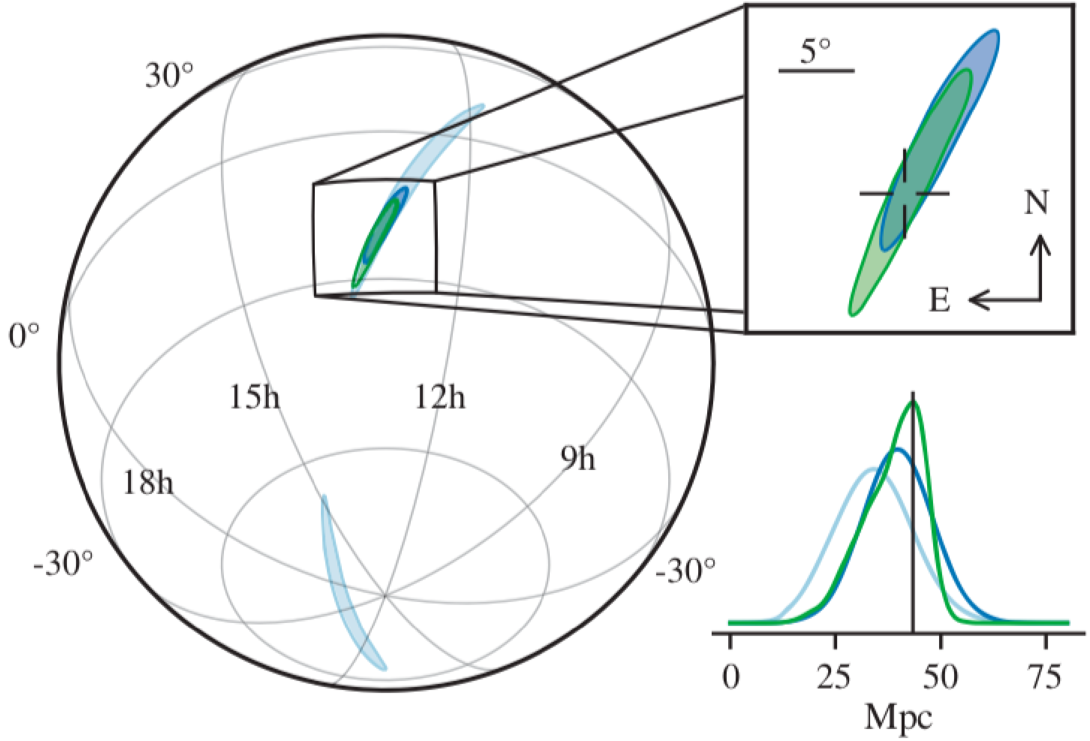

However, PE takes months for binary neutron star events.

Results

We developed a technique to utilize information from detection pipelines.

We sped up PE by a factor of $\mathcal{O}(10,000)$, which reduces the run time to less than 10 minutes.

Our method does not bias the results.

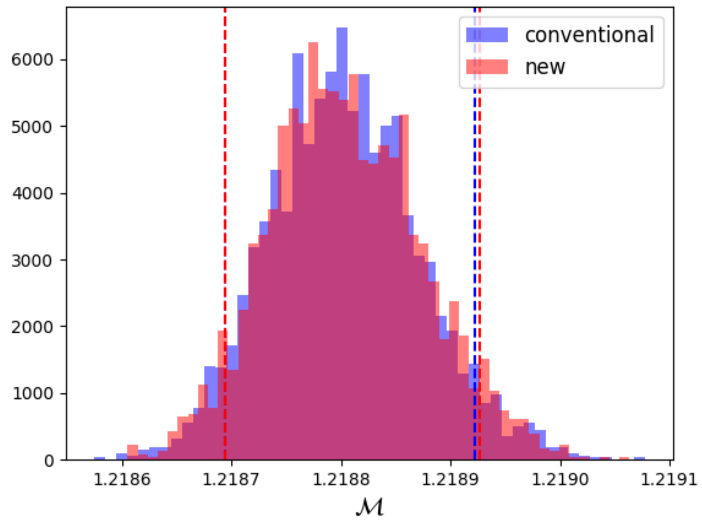

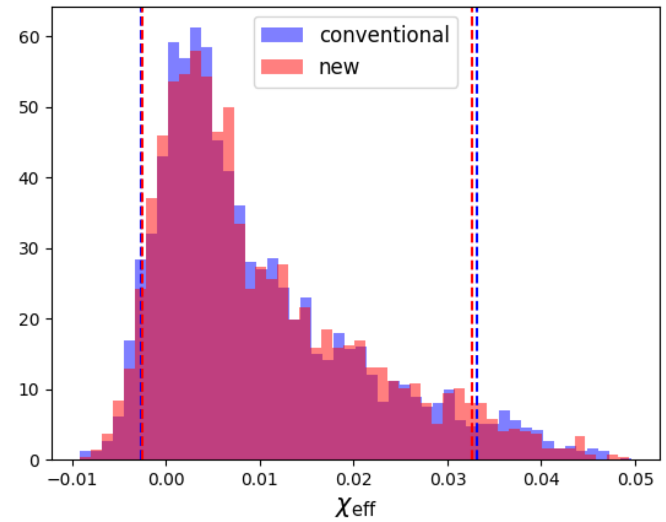

#4

An insight into the galactic hosts and environments of merging compact binary objects

Soheb Mandhai, Nial Tanvir, Gavin Lamb

Ingredients:
- Binary Population Synthesis (BPASS v2 used)
- Natal Kick
- Binary Metallicity

- Hydrodynamical Cosmological Simulation (EAGLE used)

Relative Cosmological Population of Compact Binaries

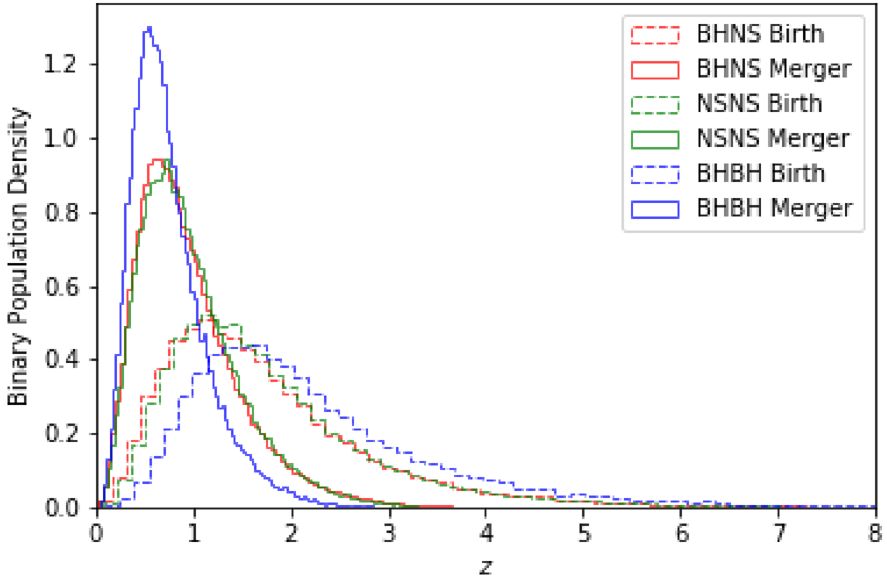

Host Galaxy Properties

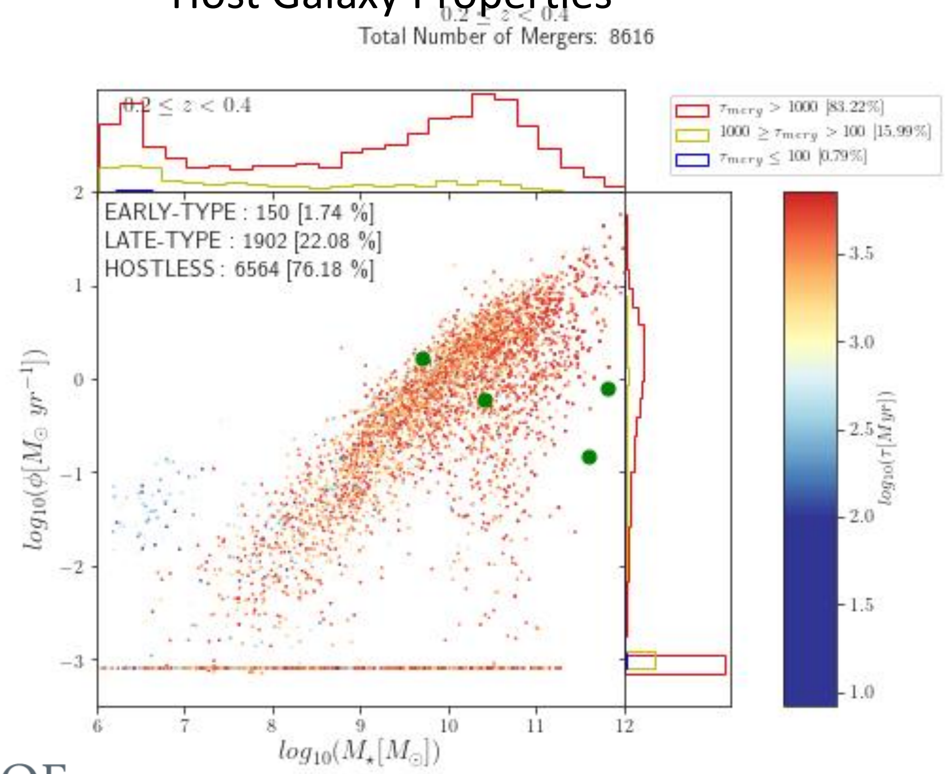

Dynamical Evolution With Kicks

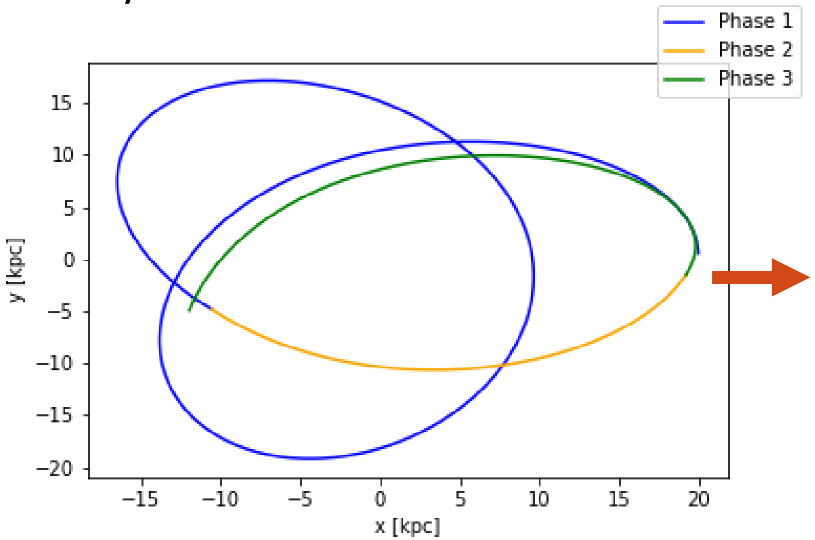

Kicked Distance Distribution

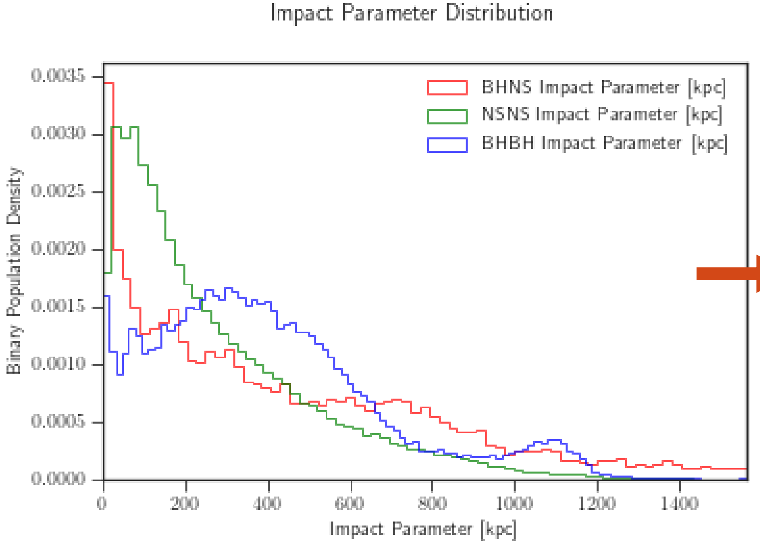

Observational Applications?

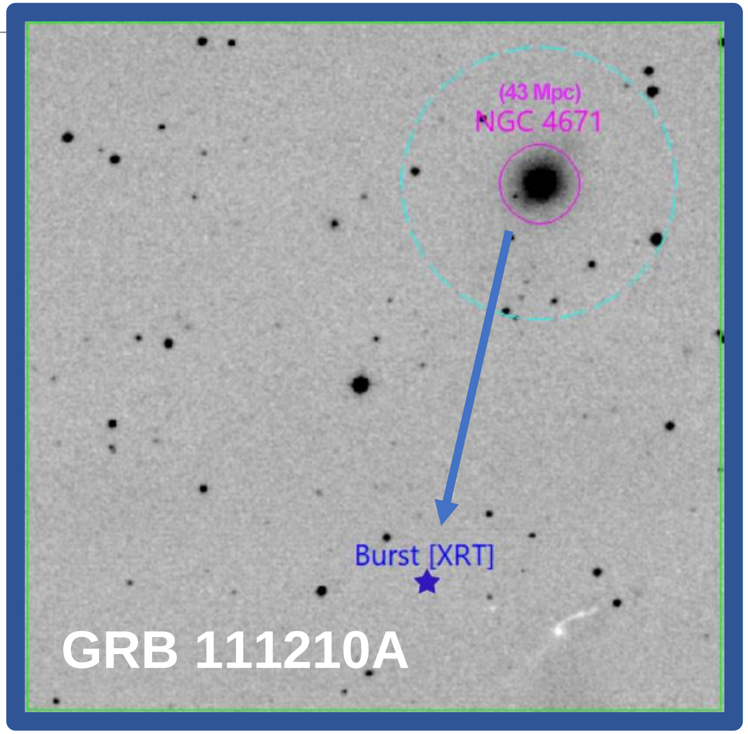

See Mandhai et al., 2018

UNIVERSITY OF LEICESTER

#5

Dispersion Measure of FRBs in a ΛCDM Universe

K. Nagamine, K. Okamoto (Osaka), B. Zhang (UNLV)

$$\mathrm{DM} = \int \frac{n_{\mathrm{e,z}}}{1+z} dl$$

$$\mathrm{DM_{tot}} = \mathrm{DM_{MW}} + \mathrm{DM_{halo}} + \mathrm{DM_{IGM}} + \mathrm{DM_{host}},$$

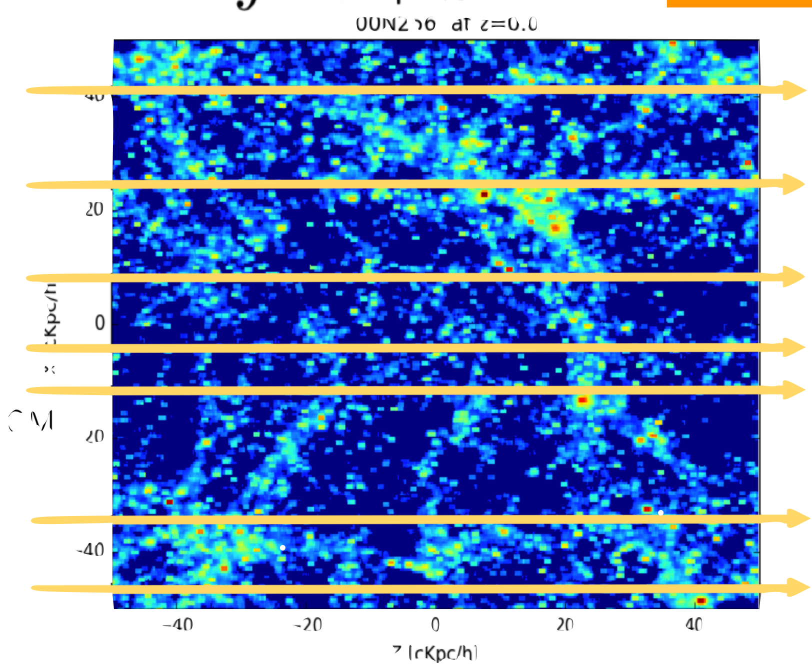

$\mathrm{DM_{MW}}$ = MW disk contrib. (NE2001, YMW16 models)

$\mathrm{DM_{halo}}$ = MW halo contrib. ≈ 30, 50-80 pc cm^{-3}

(Dolag+15; Prochaska & Zheng '19)

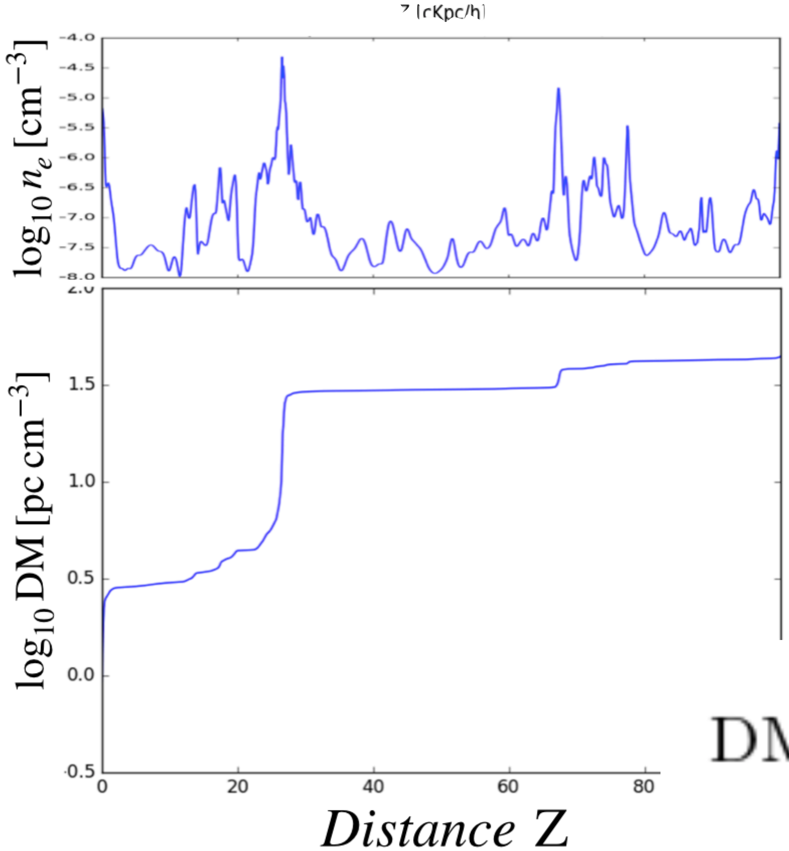

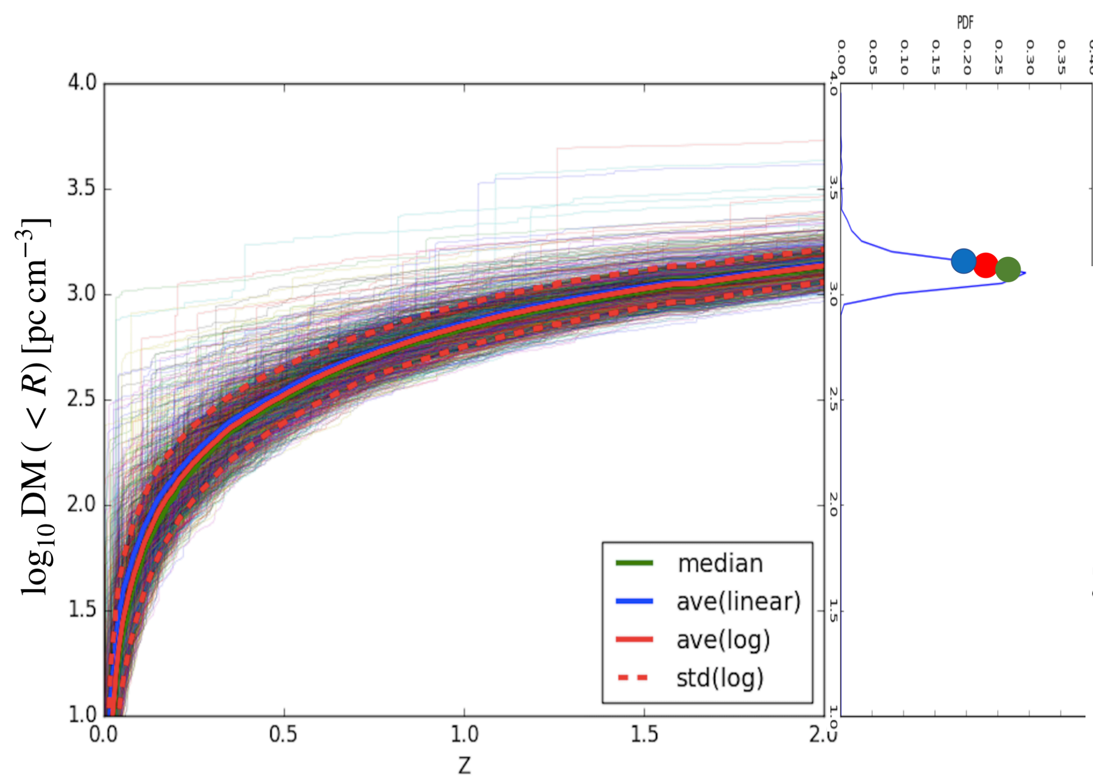

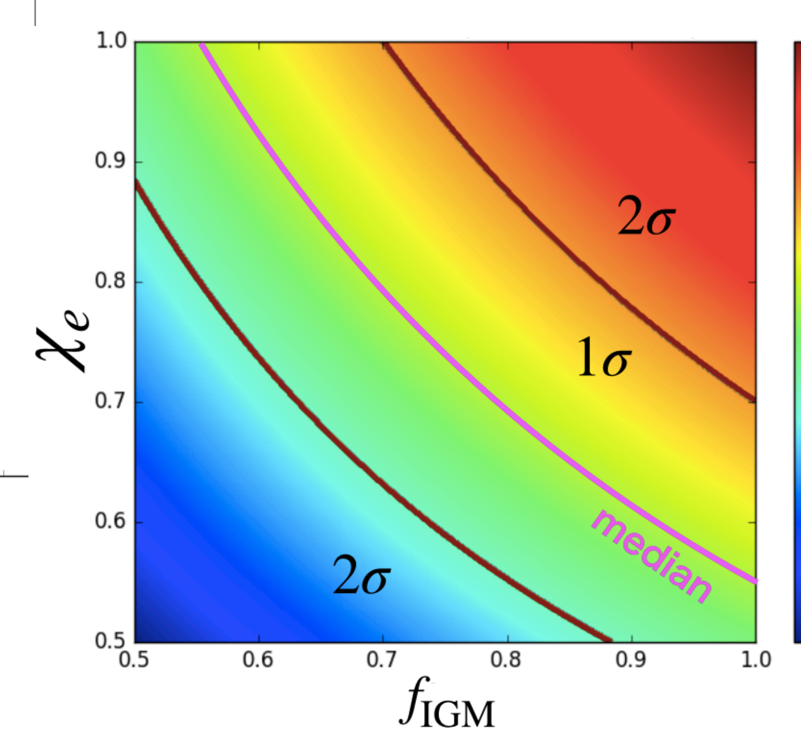

$$\mathrm{DM_{IGM}} = \frac{3cH_0\Omega_b f_{\mathrm{IGM}}}{8\pi G m_p} \int_0^z \frac{\left[\frac{3}{4}y_1\chi_{\mathrm{e,H}}(z) + \frac{1}{8}y_2\chi_{\mathrm{e,He}}(z)\right](1+z)dz}{\left[\Omega_m(1+z)^3 + \Omega_\Lambda\right]^{1/2}}.$$

THE FRB 121102 HOST IS ATYPICAL AMONG NEARBY FRBS

YE LI[1,2], BING ZHANG[3], KENTARO NAGAMINE[4,3,5], JINGJING SHI[1]

arXiv: 1906.08749

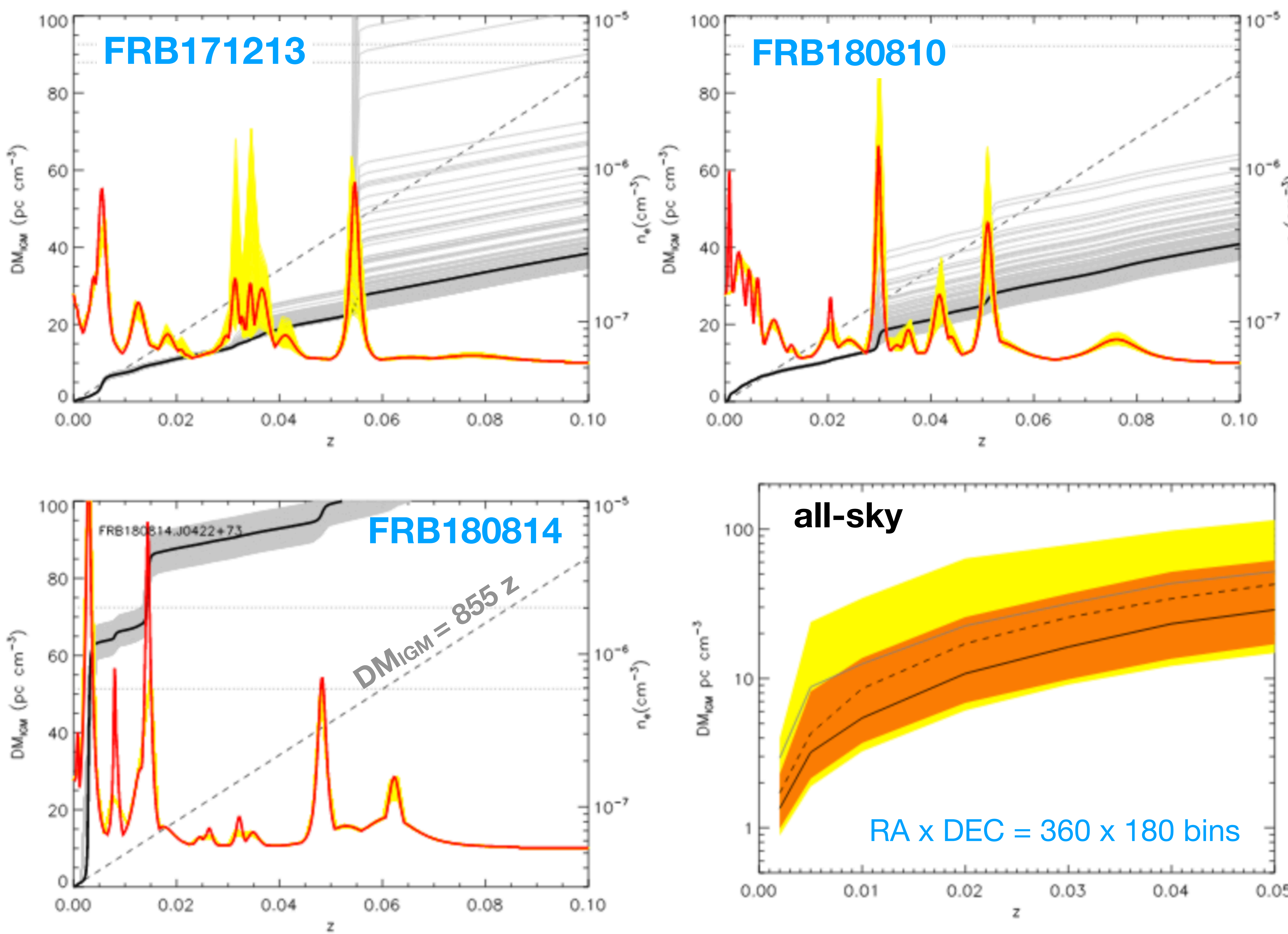

#6

#7

Identifying the host-galaxies of binary black holes with multi-messenger observations

Atsushi Nishizawa (RESCEU, U of Tokyo)

- GWs from 31 BBH have been detected so far.
(as of Sep 15, 2019)
- Astrophysical origin of BBHs are still unknown.
- O(100)/yr BBH merger events are expected in the future.

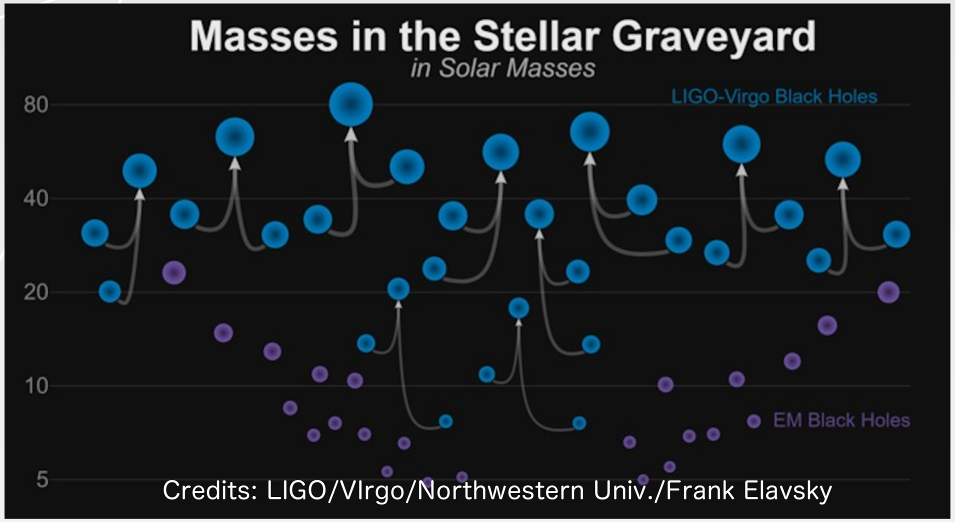

Credits: LIGO/VIrgo/Northwestern Univ./Frank Elavsky

cross-correlating sky maps

EM counterpart and distance info are not necessary.

GW events (O3 obs, Grace DB)

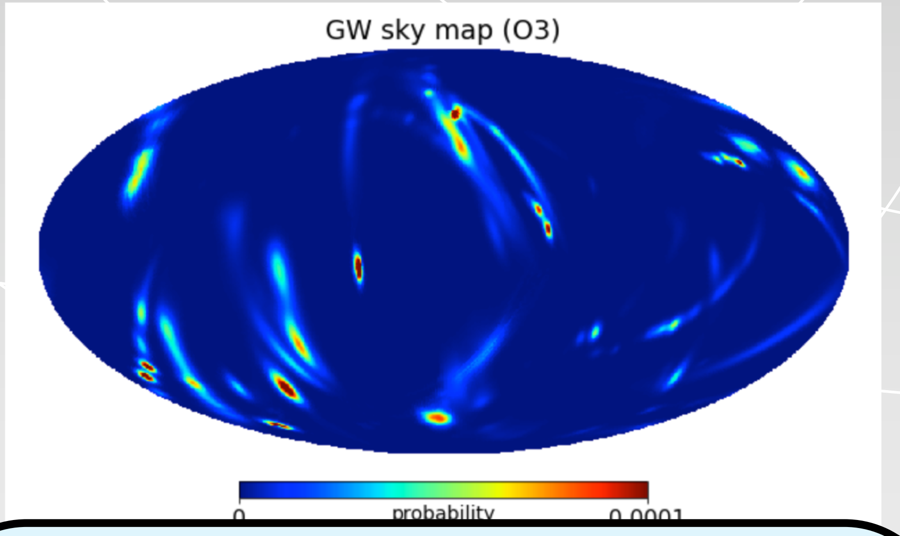

X

Asiago Supernova Catalog

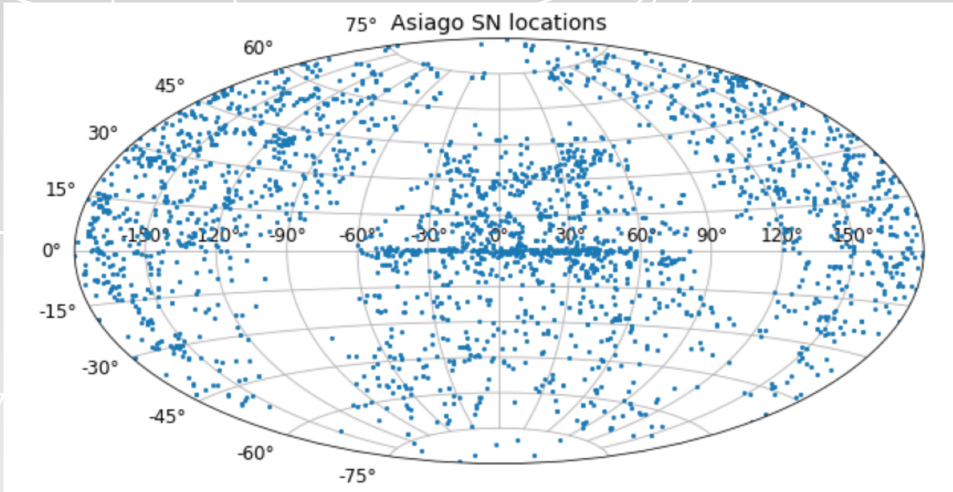

With a few – several hundreds BBHs, the clustering signal will be detected.

host galaxy properties and SN delay time

X

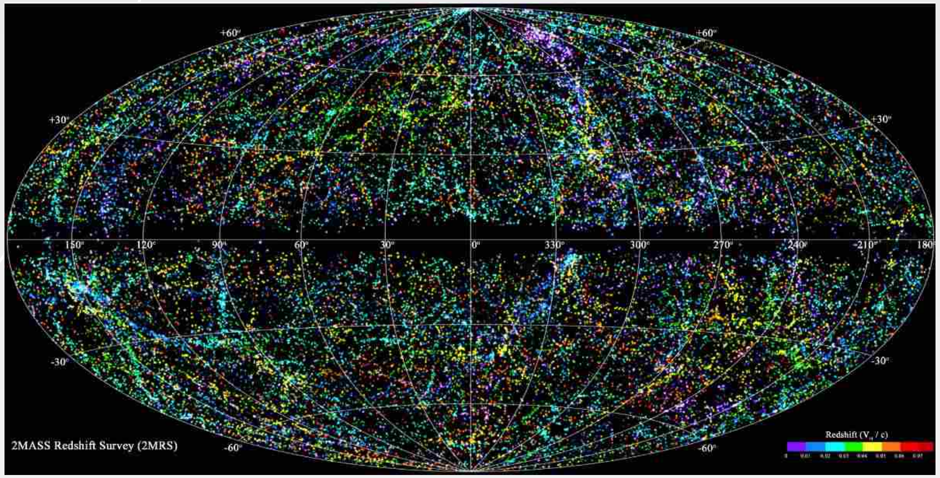

galaxy survey (2MASS)

#8

Neutrino Quantum Kinetics

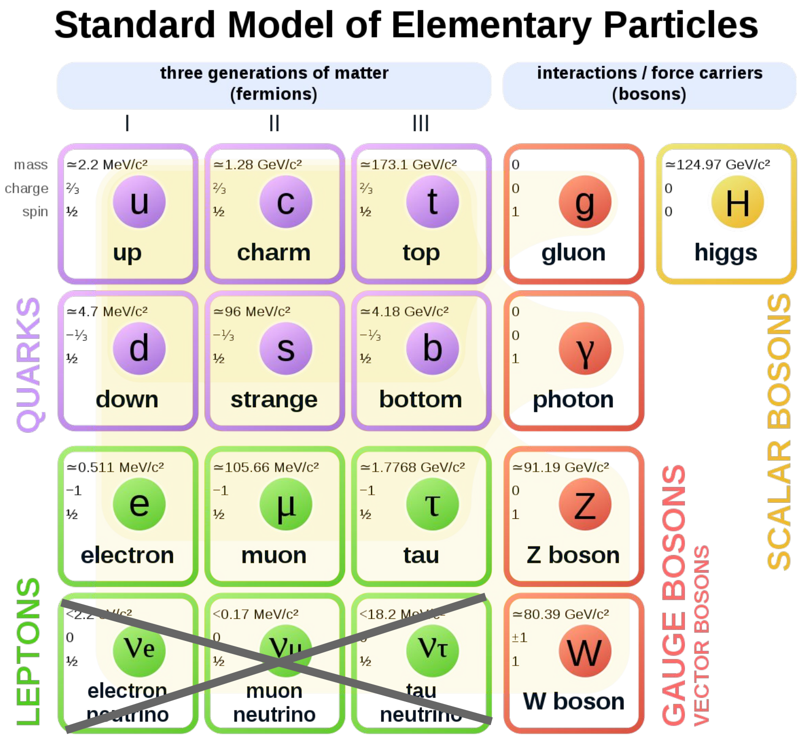

But the neutrino flavors are mixed!

(Pontecorvo 1968, Wolfenstein1978, Mikheev & Smirnov 1985)

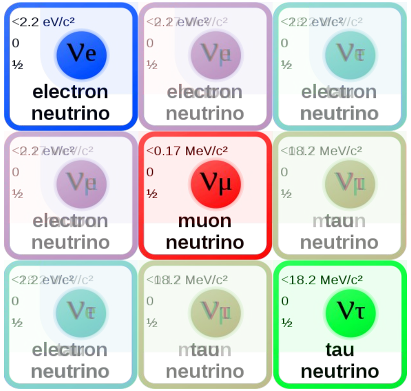

$$\frac{\partial f}{\partial t} = \{1 - f, \Pi^{+}\} - \{f, \Pi^{-}\} - i\,[\mathcal{H}, f]$$

Sherwood Richers

N3AS Postdoctoral Fellow
srichers@berkeley.edu

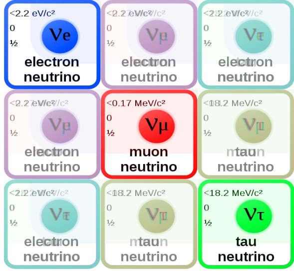

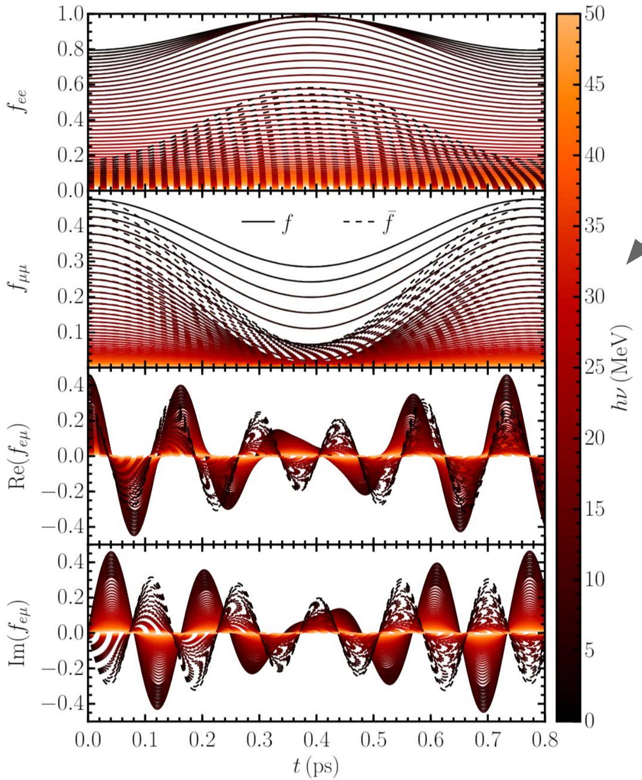

Oscillations are on extremely short timescales

Interactions take 10^7 times longer!

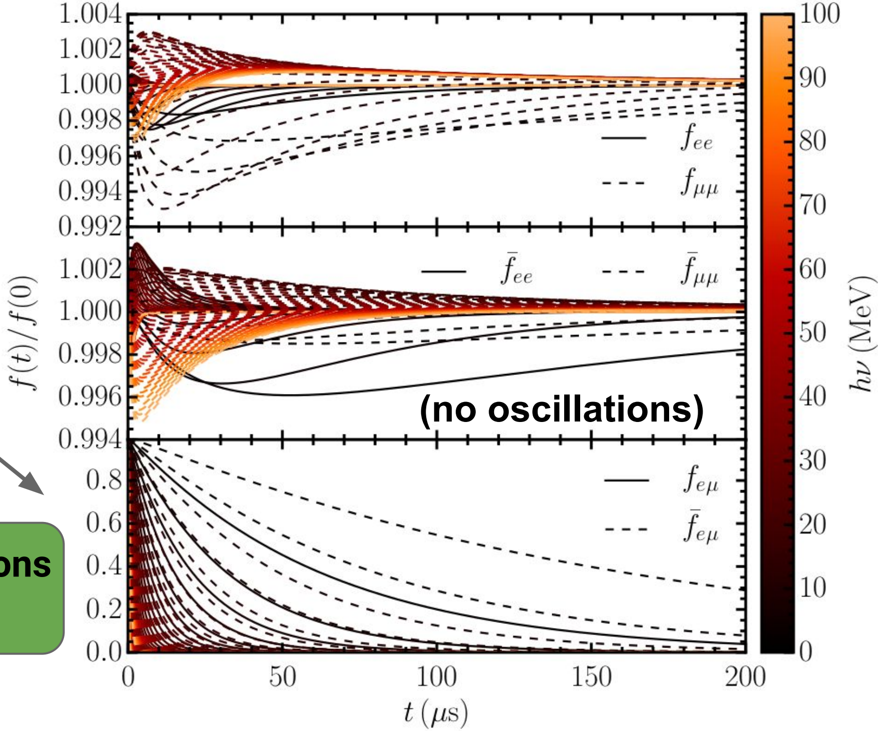

Interactions+Oscillations *at the same time*

#9

#10

#11

#12

Ring-down GW search using Auto-Regressive model

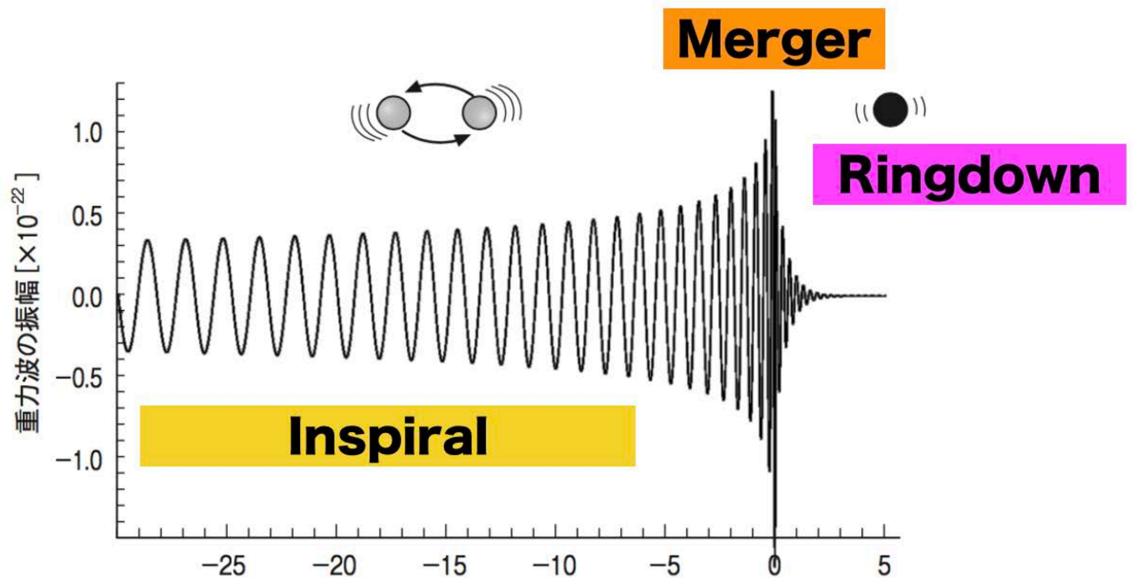

Hisaaki Shinkai (OIT)
真貝寿明（大阪工大）

AR model

$$x_n = a_1 x_{n-1} + a_2 x_{n-2} + \cdots + a_M x_{n-M} + \varepsilon = \sum_{j=1}^{M} a_j x_{n-j} + \varepsilon$$

power spectrum

$$p(f) = \frac{\sigma^2}{\left| 1 - \sum_{j=1}^{M} a_j e^{-I 2\pi j f \Delta t} \right|^2}$$

characteristic eq.

$$f(z) = 1 - \sum_{j=1}^{M} a_j z^j = 0$$

$|z_k|$ says amplitude,
$\arg(z_k)$ says frequency.

GW150914

LIGO paper

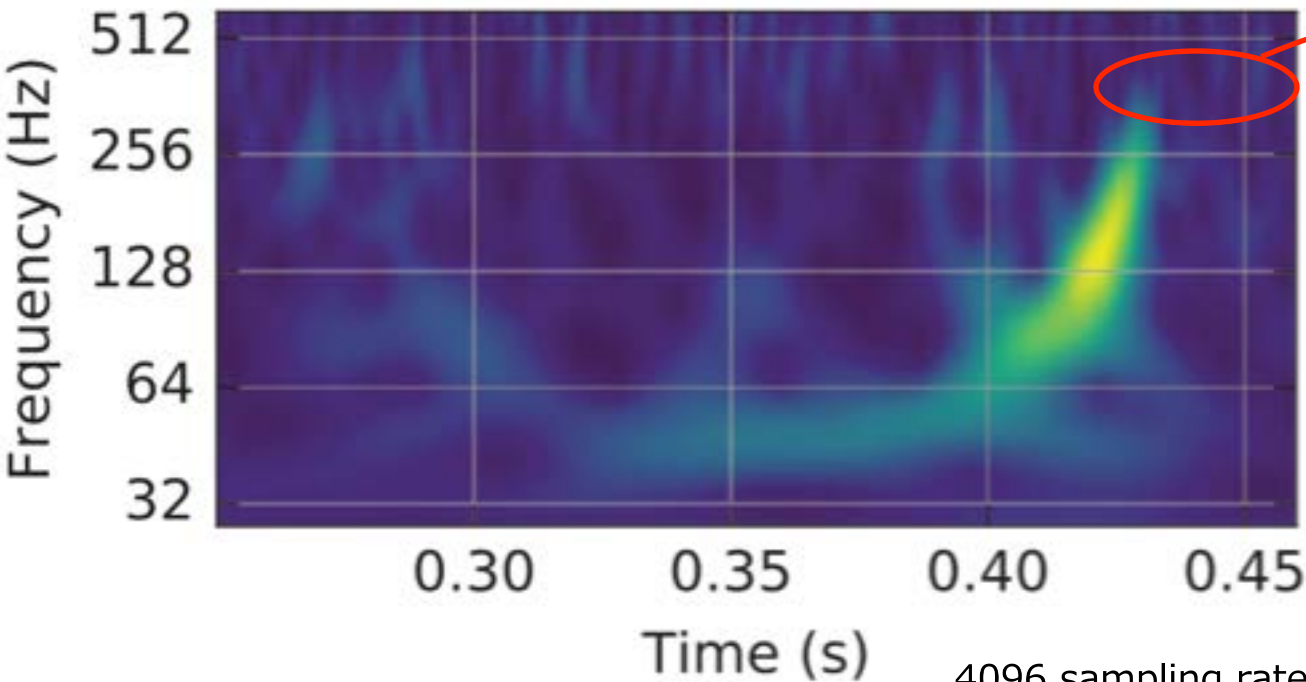

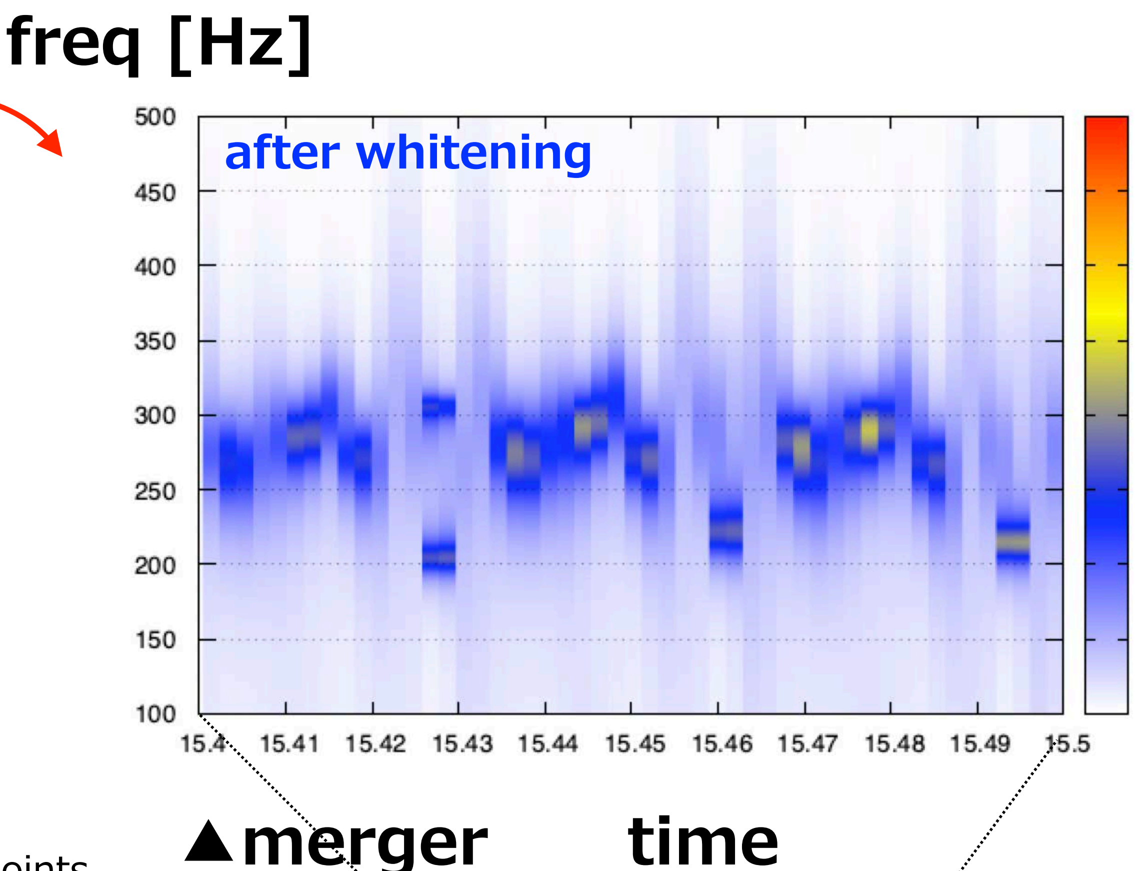

4096 sampling rate
150-450 Hz filter
1 segment = 1/64 sec= 64 points
1 shift = 1/512 sec = 8 points

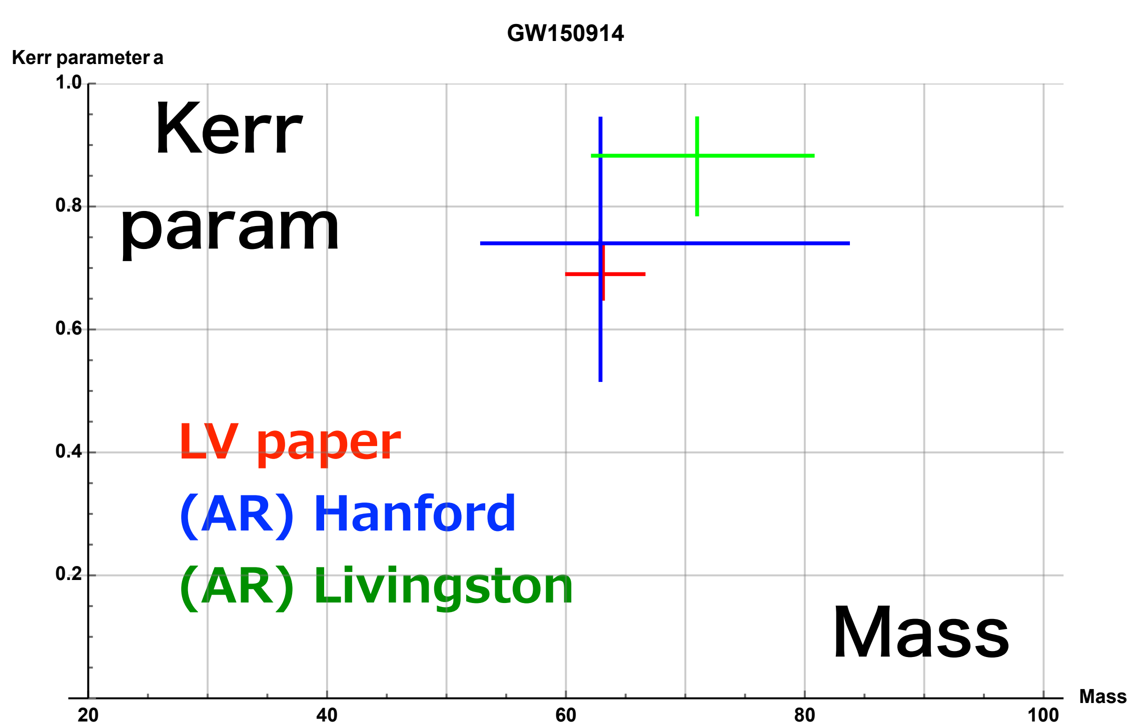

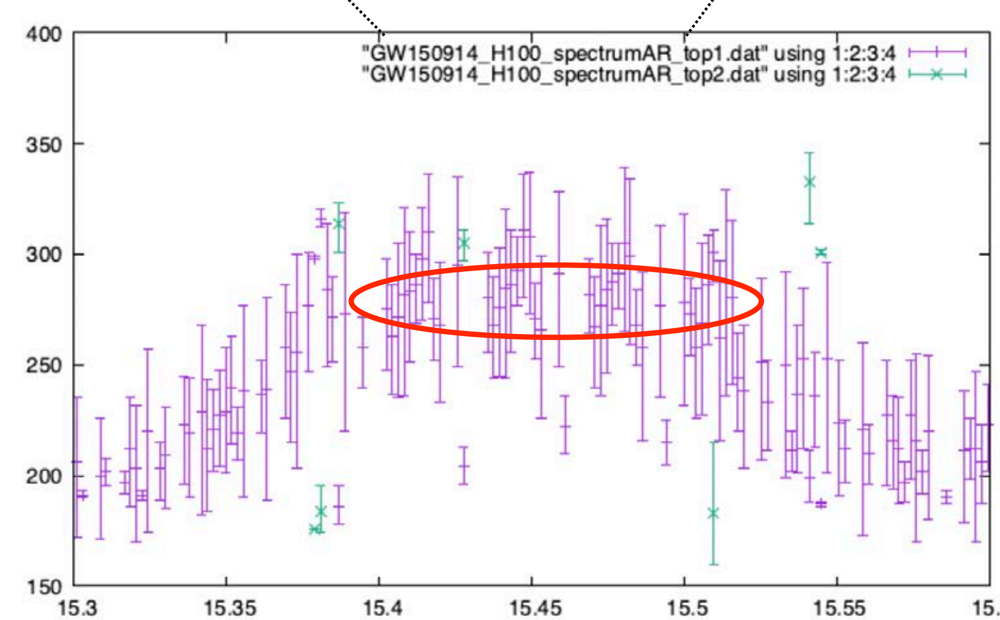

#13

#14

Follow-up observations of gravitational wave sources with Subaru/Hyper Suprime–Cam and future plan

Takayuki Ohgami (Konan Univ.)

KONAN UNIVERSITY

Several events of interest so far

- S190408an (BBH, 1473Mpc, 387deg^2)
- S190412m (BBH, 812Mpc, 156deg^2)
- S190425z (BNS, 156Mpc, 7461deg^2)
- S190426c (BNS[49%], NSBH[13%], 377Mpc, 1131deg^2)
- S190510g (BNS[98%] -> Terrestrial[58%], BNS[42%], 227Mpc, 1166deg^2)
- S190521r (BBH[99%], 1136Mpc, 488deg^2)
- S190814bv (NSBH[99%], 267Mpc, 23deg^2)

Subaru/Hyper Suprime Cam

- Diameter:8.2m, FoV:1.77deg^2, ~900M pixels
- The most powerful camera in the world

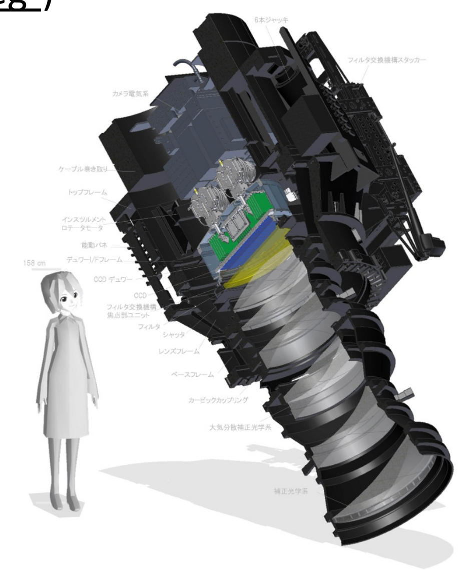

GW170817

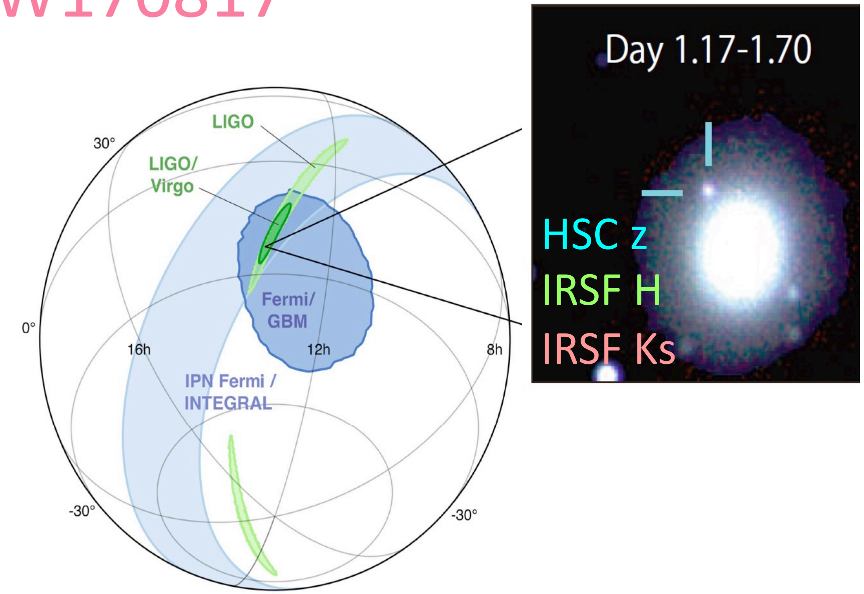

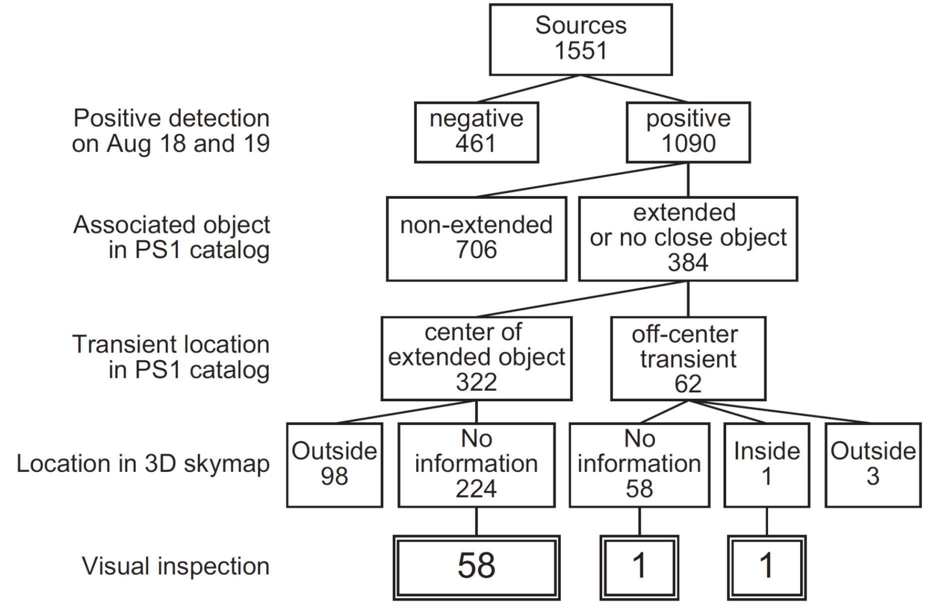

$$P_{3\mathrm{D}}(\lambda_j, m_j) = \frac{\int_{D_{\mathrm{mean}}-3\sigma_D}^{D_{\mathrm{mean}}+3\sigma_D} \phi(\lambda[\lambda_j, D], M[m_j, D]) A(D) dD}{\int_0^\infty \phi(\lambda[\lambda_j, D], M[m_j, D]) A(D) dD}$$

S190510g (LVC alert)

- Preliminary alert: 13:03 May 10, 2019 (JST) 268Mpc
- Initial alert: 14:24 May 10, 2019 (JST)
- HSC observation start: 14:46 May 10, 2019 (JST)
- Update Alert: 19:23 May, 10, 2019 (JST)
- GCN 24450
  LIGO/Virgo S190510g: HSC Y-band follow-up observation

#15

Evolution tracks of massive stars under extreme metal poor environments and its application

Ataru Tanikawa (The University of Tokyo)

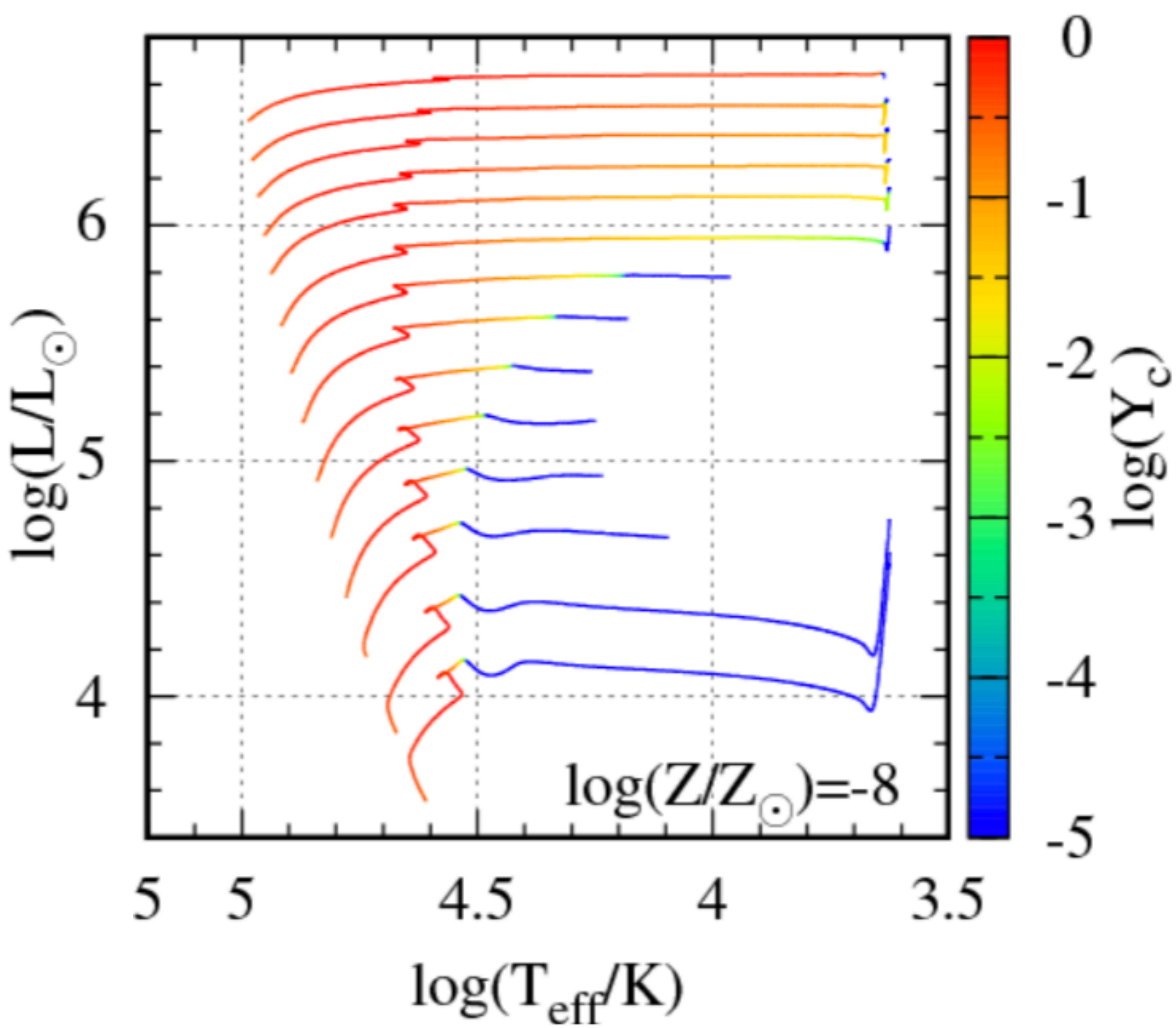

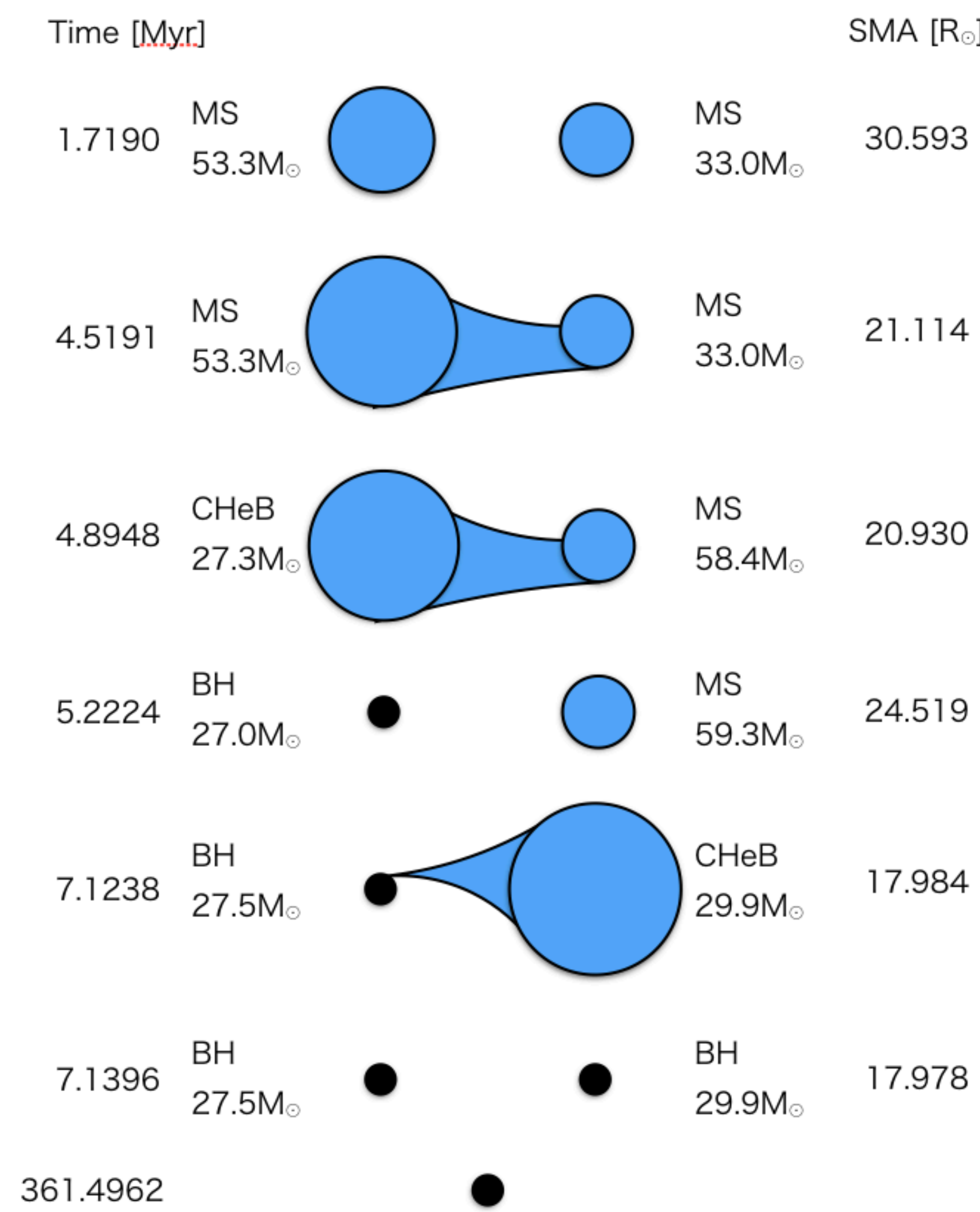

Tanikawa et al. (2019, arXiv:1906.06641)

- Support for SSE/BSE/NBODY4/NBODY6++GPU
- Stellar evolution tracks for $\log\left(Z/Z_{\odot}\right) = -2, -4, -5, -6, -8$
- Mass range: $8 \leq M/M_{\odot} \leq 160$, possibly $8 \leq M/M_{\odot} \lesssim 200$
- Stellar wind implemented by Belczynski et al. (2010) with modification of Kinugawa, Yamaguchi (2018) for EMP stars
- PPISN and PISN modeled by Belczynski et al. (2016)

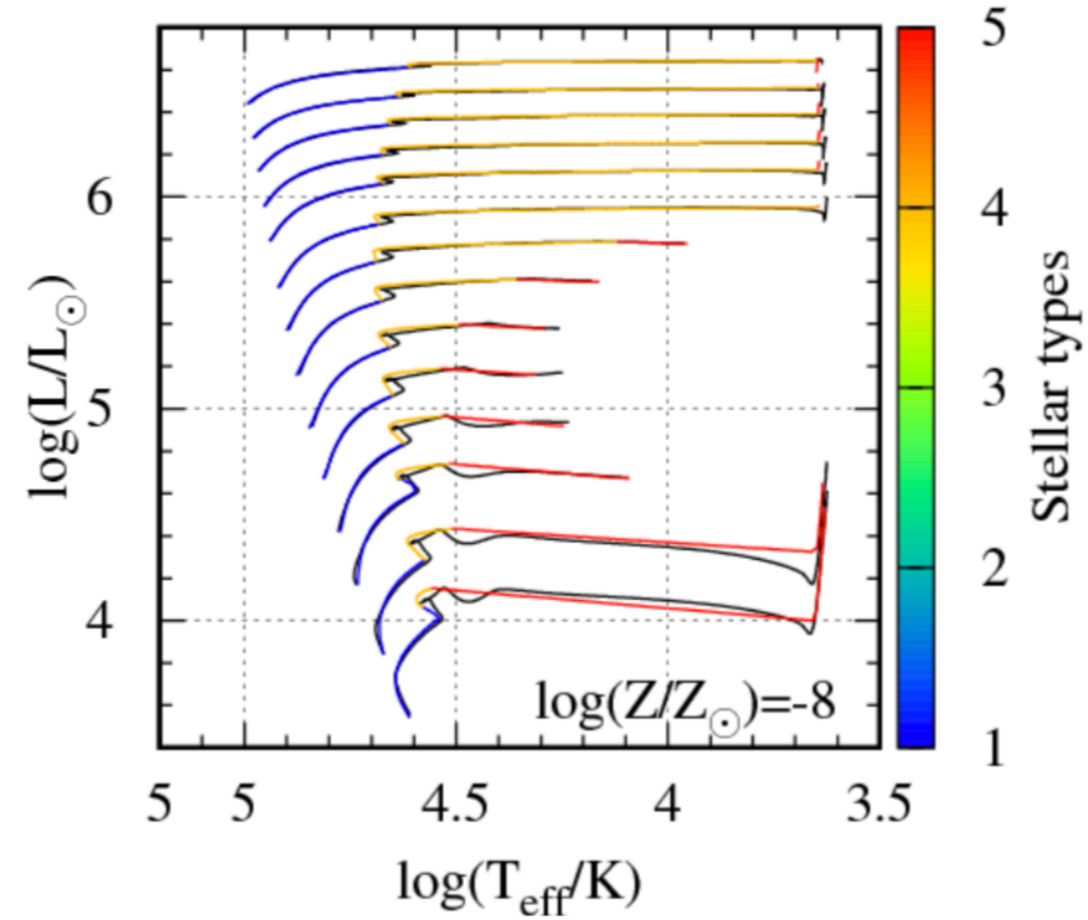

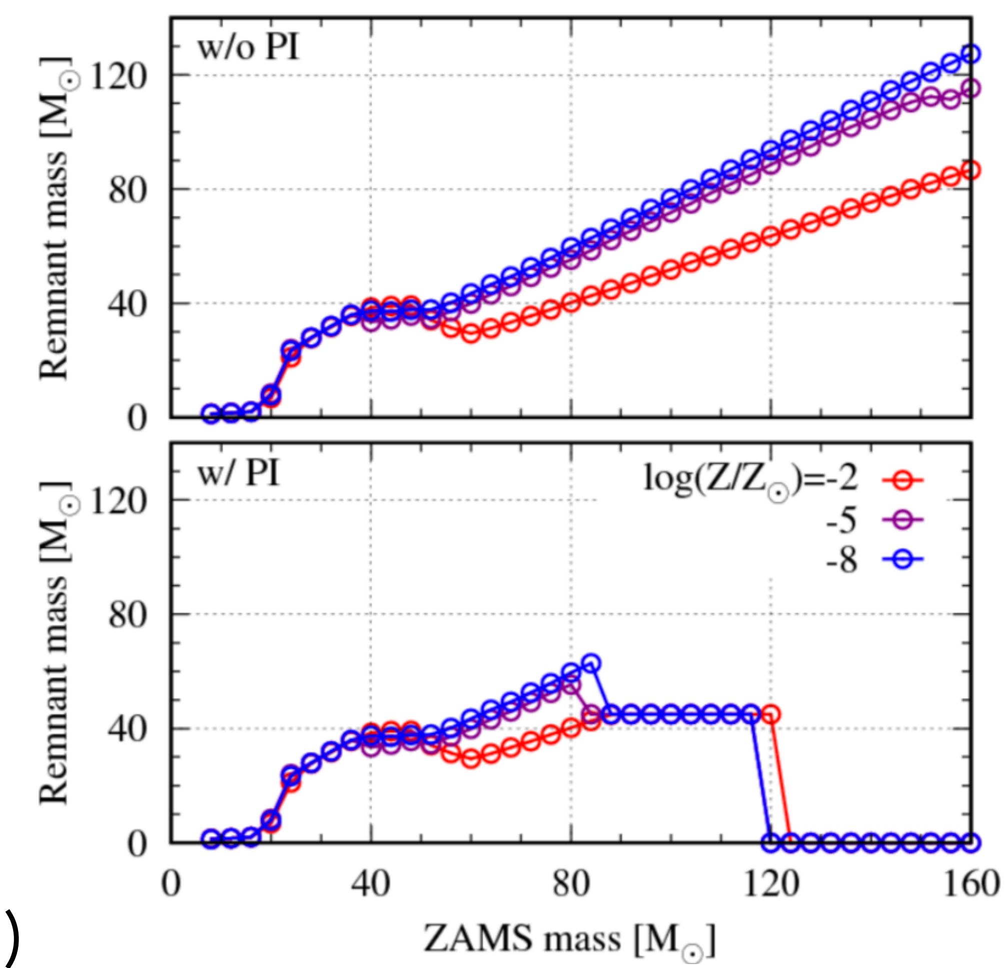

Tanikawa et al. (2019, arXiv:1906.06641)

#16

Black hole ringdown analysis with KAGRA upgrade plan

Nami Uchikata, Kazuki Sakai, Hiroyuki Nakano, Tatsuya Narikawa, Hirotaka Takahashi

We analyze black hole QNM for three proposed KAGRA upgrade plans.

We use numerical waveforms that are composed of two modes.

$$(l, m) = (2,2), (3,3)$$

We estimate the frequency and the quality factor for each mode.

$$e^{-\frac{\pi f t}{Q}} \cos(2\pi f t)$$

We compare the results for each sensitivity curves.

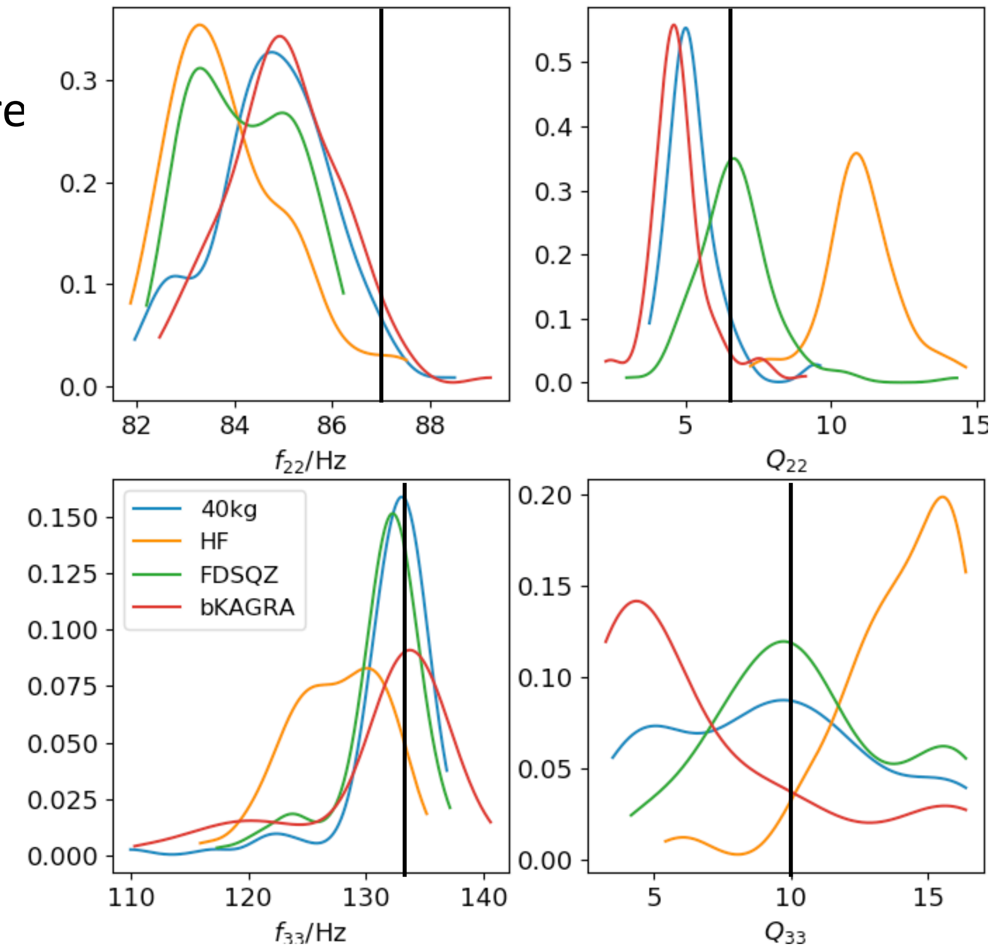

#17

#18

Energy function, formation rate, and low-metallicity environment of fast radio bursts

G. Q. Zhang and F. Y. Wang

2019, Kyoto

FRB 121102: $12 + \log\left(\frac{O}{H}\right) < 8.4$

FRB 190523: $0.3(2)\ Z_{\odot}$

Collect FRB：

28 Parkes FRBs & 23 ASKAP FRBs

Whether FRBs were born in metal-poor galaxies?

Derive redshift from DM and redshift cumulative distribution.

$$N(<z) = A\int_0^z \rho_{\rm FRB}(z)\left[\int_0^1 \eta(\varepsilon)\int_{E_{\rm th}/\varepsilon}^{E_{\rm max}} \Phi(E){\rm d}E{\rm d}\varepsilon\right] \times \frac{{\rm d}V(z)}{1+z},$$

- Metallicity

$$\Psi(Z,z) = \frac{\widehat{\Gamma}\left[\alpha+2, (Z/Z_{\odot})^{\xi}\, 10^{0.15\xi z}\right]}{\Gamma(\alpha+2)},$$

- Formation rate of FRBs
  - With Time delay

$$\rho_{FRB}(z) \propto R(z,\tau)\Psi(Z,z)$$

  - Without Time delay

$$\rho_{FRB}(z) \propto \rho_{CSFR}(z)\Psi(Z,z)$$

- Energy distribution

$$\Phi(E) \propto E^{-\gamma}$$

	Parkes	ASKAP	Parkes	ASKAP
τ (Gyr)	$2.77^{+2.86}_{-1.90}$	$5.50^{+3.01}_{-3.62}$		
γ	$1.63^{+0.32}_{-0.25}$	$2.07^{+0.14}_{-0.14}$	$2.37^{+0.12}_{-0.16}$	$2.40^{+0.08}_{-0.08}$
$Z(Z_{\odot})$	$0.46^{+0.35}_{-0.31}$	$0.52^{+0.32}_{-0.34}$	$0.52^{+0.34}_{-0.34}$	$0.52^{+0.32}_{-0.34}$
p-value	0.41	0.92	0.55	0.78

Zhang & Wang, 2019, MNRAS, 487, 3672

- We find the metallicity is low in all the cases.
- The γ may help us distinguish between the two models (compact binary merger or core-collaspse).
- The energy distribution of repeater (FRB 121102) also shows $\gamma \sim 1.8$. Similarity between repeaters and non repeaters.

#19

Population of black hole quasi-normal modes for ground-based detectors

- Testing GR with the black hole ringdown
- Perturbed Kerr black hole has characteristic spectrum of discrete modes
- No-hair theorem: $\mathcal{B} = \mathcal{B}(M, a)$ $\rightarrow$ 2 parameters determine all modes
- Compare multiple modes' parameters $\omega_{\ell m}$, $\tau_{\ell m}$

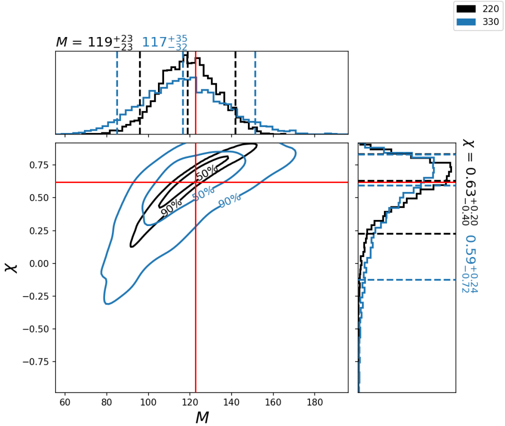

Population of black hole quasi-normal modes for ground-based detectors

- Simulate population of ringdown signals based on LIGO analyses
- Perform Bayesian inference:
  - Find signals with two detectable modes
  - Resolve mode parameters and test compatibility
- Calculate rates for ground-based detector networks

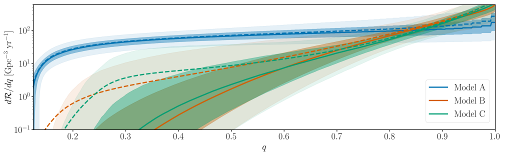

arXiv:1811.12940

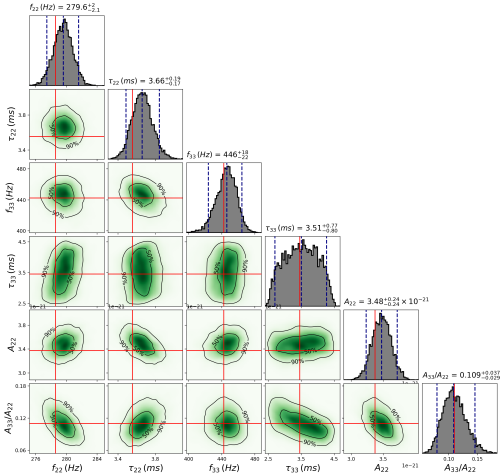

#20

CDF-S XT2 as a Newly-discovered GW Counterpart

Di Xiao, Bin-Bin Zhang & Zi-Gao Dai,
Nanjing University, China

Observation of X-ray transient CDF-S XT2

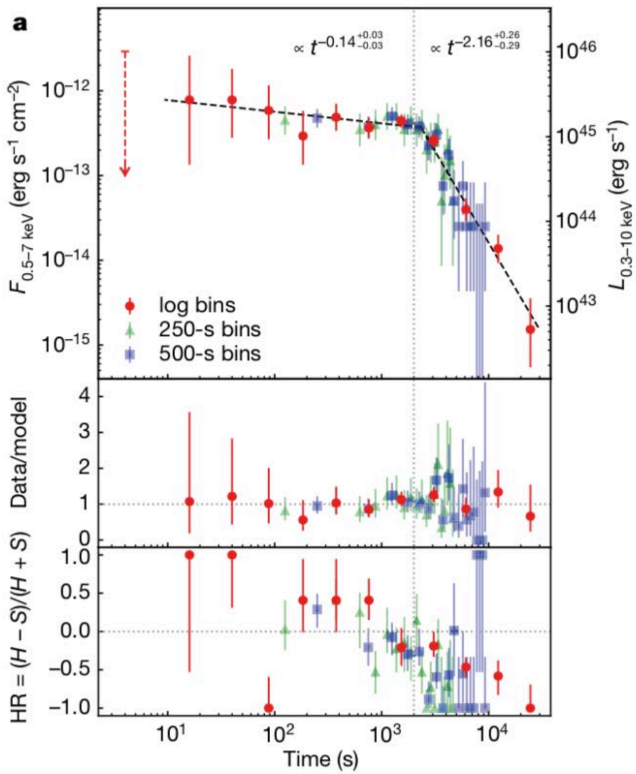

Xue et al. 2019

Schematic picture of EM counterparts if central remnant is a massive NS after BNS merger

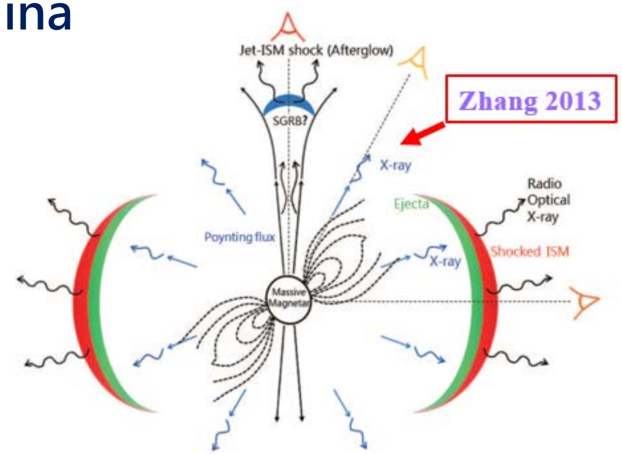

Gao et al. 2013; Sun et al. 2017

Emission mechanism: Magnetar wind Internal Gradual MAgnetic Dissipation (MIGMAD)

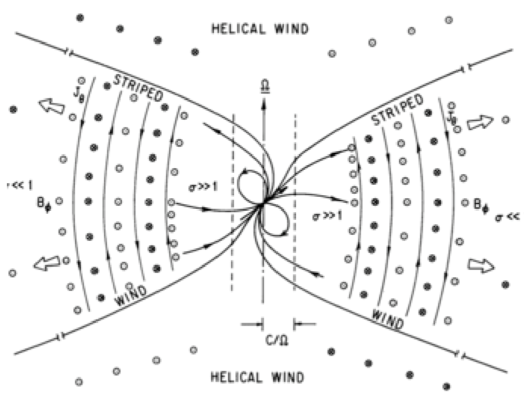

Coroniti 1990

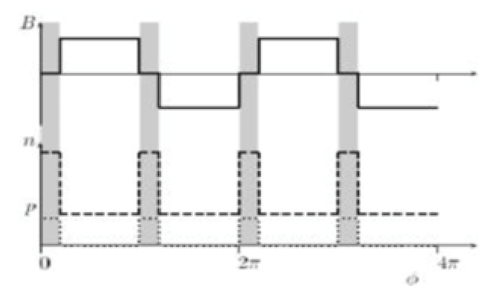

"Striped Wind" Configuration

CDF-S XT2 as a Newly-discovered GW Counterpart

Results

X-ray Radiation efficiency

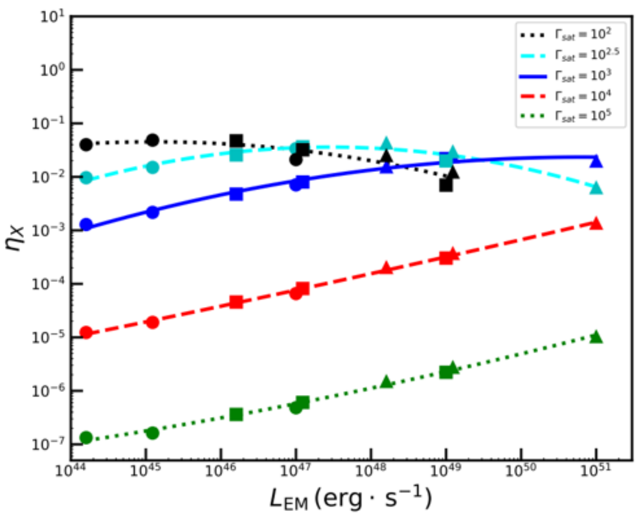

Xiao & Dai 2019 ApJ

Light-curve fitting

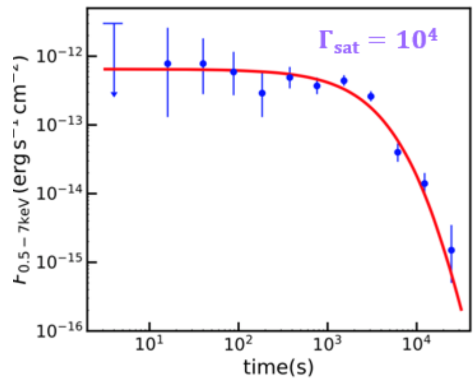

The Best-fitting Parameters for Five Different Γ_{sat}

	Best-fitting values			
	t_0	$\log L_0$	n	$\log \tau$
$\Gamma_{sat} = 10^2$	$72.72^{+10.77}_{-55.26}$	$46.14^{+0.09}_{-0.11}$	$1.59^{+0.66}_{-0.20}$	$4.12^{+0.23}_{-0.48}$
$\Gamma_{sat} = 10^{2.5}$	$74.53^{+9.51}_{-59.64}$	$46.24^{+0.08}_{-0.08}$	$1.76^{+0.86}_{-0.30}$	$4.13^{+0.26}_{-0.48}$
$\Gamma_{sat} = 10^3$	$61.76^{+23.07}_{-44.97}$	$46.96^{+0.07}_{-0.07}$	$1.83^{+0.84}_{-0.32}$	$4.12^{+0.26}_{-0.45}$
$\Gamma_{sat} = 10^4$	$73.47^{+12.11}_{-57.33}$	$48.60^{+0.06}_{-0.07}$	$1.69^{+0.81}_{-0.30}$	$4.22^{+0.30}_{-0.46}$
$\Gamma_{sat} = 10^5$	$92.33^{+7.65}_{-33.97}$	$50.21^{+0.06}_{-0.07}$	$1.72^{+0.84}_{-0.30}$	$4.22^{+0.28}_{-0.47}$

Xiao, Zhang & Dai 2019 ApJL

X-ray photon index: from 1.57 (<2000s) to 2.53 (>2000s)

Slow cooling regime: $F_\nu \propto \nu^{-0.5}$ to $F_\nu \propto \nu^{-(p-1)/2}$

Table 2

The Upper Limits of Initial Spin Period and Magnetic Field Strength for Five Different Γ_{sat}

	P_0 (in ms)	B (in Gauss)
$\Gamma_{sat} = 10^2$	$14.35^{+13.67}_{-4.50}$	$7.68^{+21.62}_{-4.06} \times 10^{15}$
$\Gamma_{sat} = 10^{2.5}$	$12.82^{+11.80}_{-4.17}$	$6.83^{+18.33}_{-3.72} \times 10^{15}$
$\Gamma_{sat} = 10^3$	$5.64^{+4.58}_{-1.78}$	$3.04^{+6.92}_{-1.61} \times 10^{15}$
$\Gamma_{sat} = 10^4$	$0.76^{+0.64}_{-0.25}$	$3.63^{+8.78}_{-2.02} \times 10^{14}$
$\Gamma_{sat} = 10^5$	$0.12^{+0.10}_{-0.04}$	$5.73^{+14.05}_{-3.12} \times 10^{13}$

Typical values of a magnetar formed by NS mergers indicated by numerical simulations

Paper link:
https://iopscience.iop.org/article/10.3847/2041-8213/ab2980

Xiao, Zhang & Dai 2019 ApJL

#21

#22

#23

No. 23

Power spectrum of Primordial Tensor Perturbations in double inflationary scenario with a break

Shi Pi, Misao Sasaki, YZ, JCAP 1906 (2019) 049, arxiv:1904.06304 [gr-qc]

We considered the case with a break during inflation and calculated the **Primordial Tensor Perturbations**.

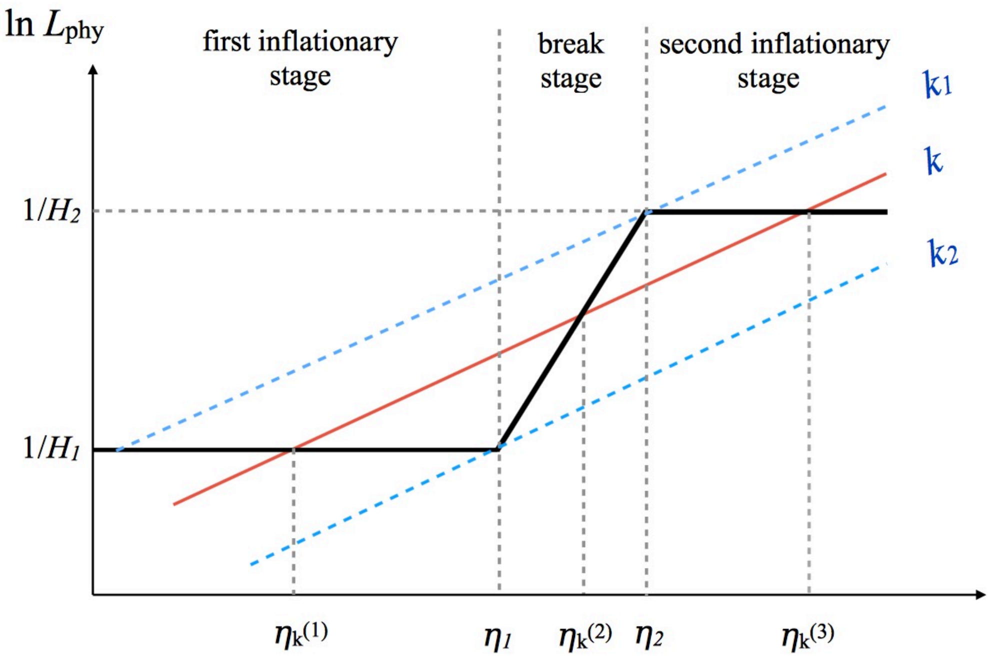

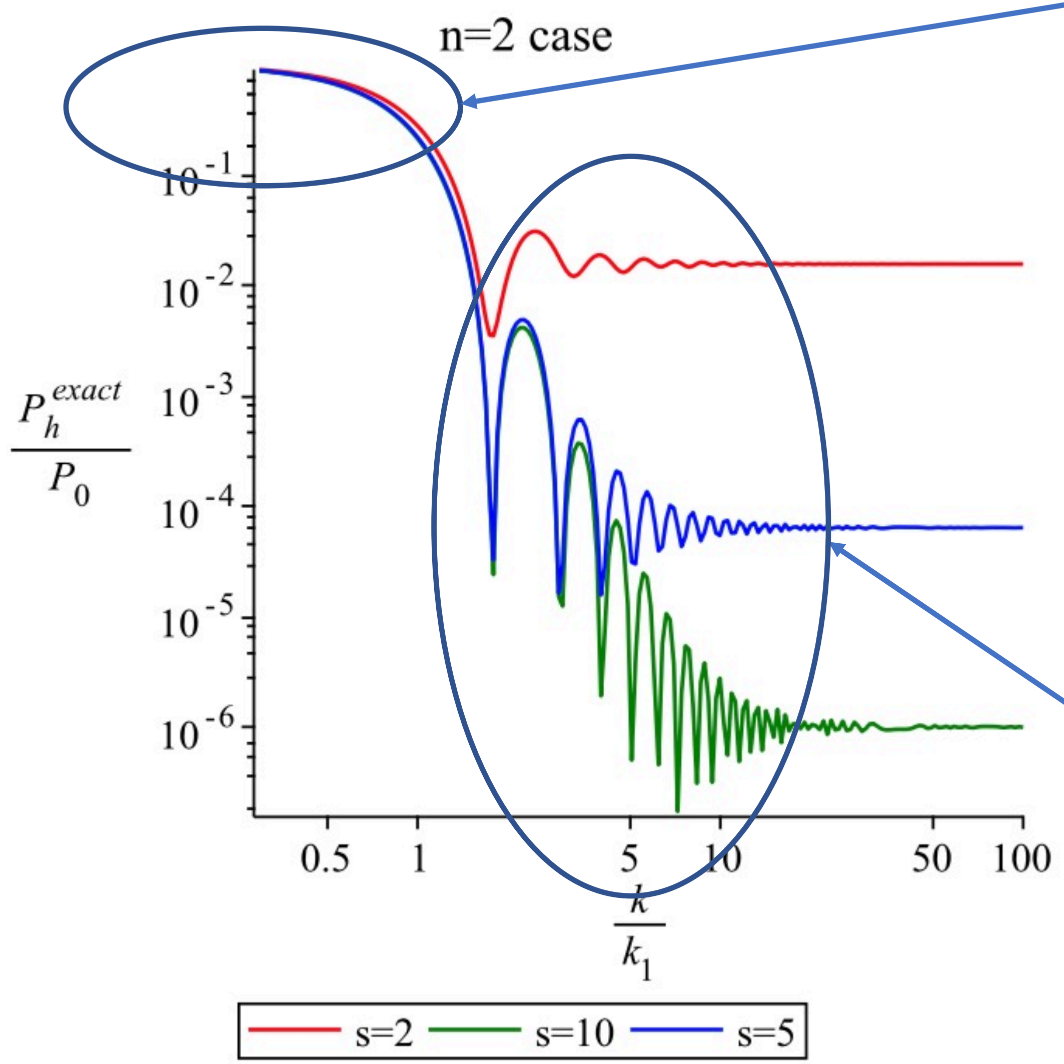

Decay of amplitude even outside the horizon

Oscillational behavior and no enhancement of amplitude

#24

Gravitational-wave merging events from the stellar mass binary black holes around the massive black hole in a galactic nucleus

Zhang Fupeng(张福鹏), Guangzhou University

Shao Lijing (PKU), Zhu Weishan(SYSU)

ApJ 2019, 877, 87

- **We aim to build a comprehensive Monte-Carlo numerical method to study the evolution of stellar mass binary black holes (BBHs) in a galactic nucleus**
  - ✓ **Two body relaxation: Fokker-Planck diffuse equation**
  - ✓ **Binary-Single Encounters，Kozai-Lidov (KL) Oscillations，Gravitational Wave orbital decay, Tidal force of the MBH**

Evolutions of the outer orbit of BBHs

Distance to the MBH

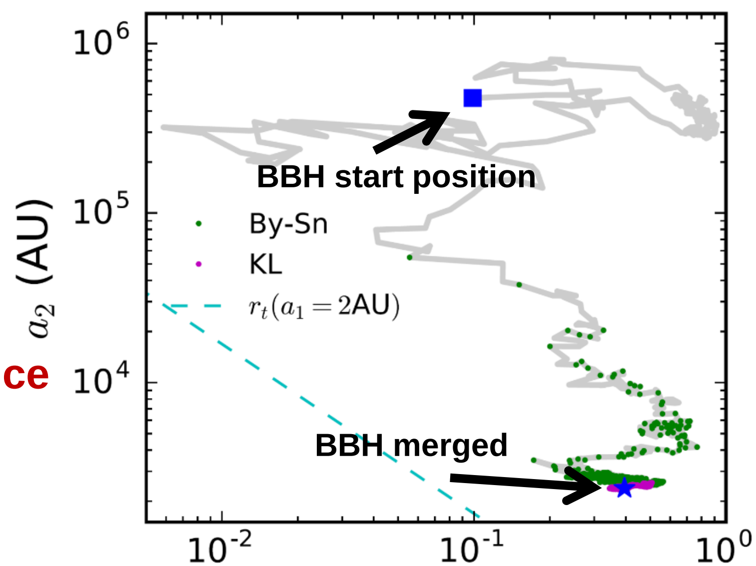

1 - eccentricity of outer orbit

Evolution of the inner orbit of BBHs

Semimajor axis of the inner orbit

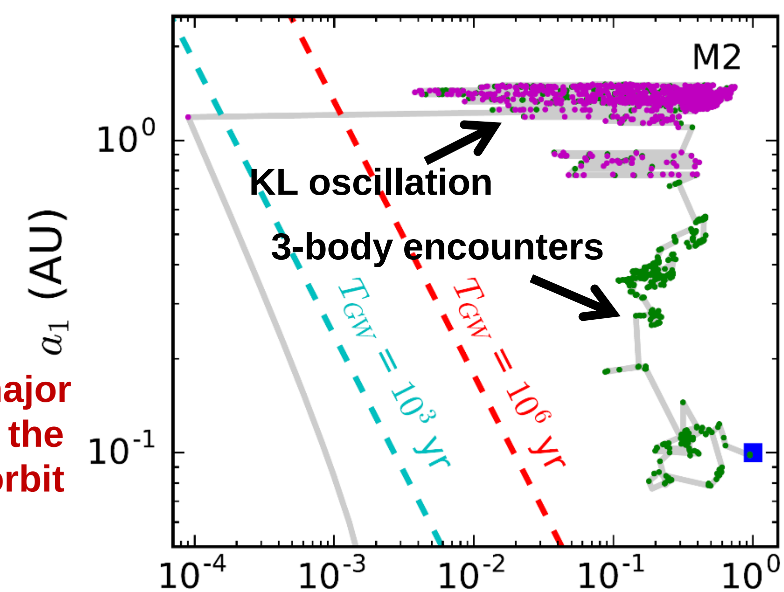

1- eccentricity of inner orbit

Results and predictions

- ✓ **Dynamics of BBHs:** BBH-single star encounters is another channel of merging BBHs
- ✓ **The distribution of BBH orbits**
- ✓ **The merging event rate of BBHs in local universe: 1-10** Gpc^{-3} yr^{-1}
- ✓ **Eccentricity distribution of the merging BBHs in the LIGO band:**
  3-10% e_{10Hz} >0.01， much higher than those in globular cluster and field regions
- ✓ **Other properties of the merging BBHs:**
  Most BBHs merger are within galactic nuclei with MBH <10^8 Msun

Number density distribution of BBHs

Distribution function

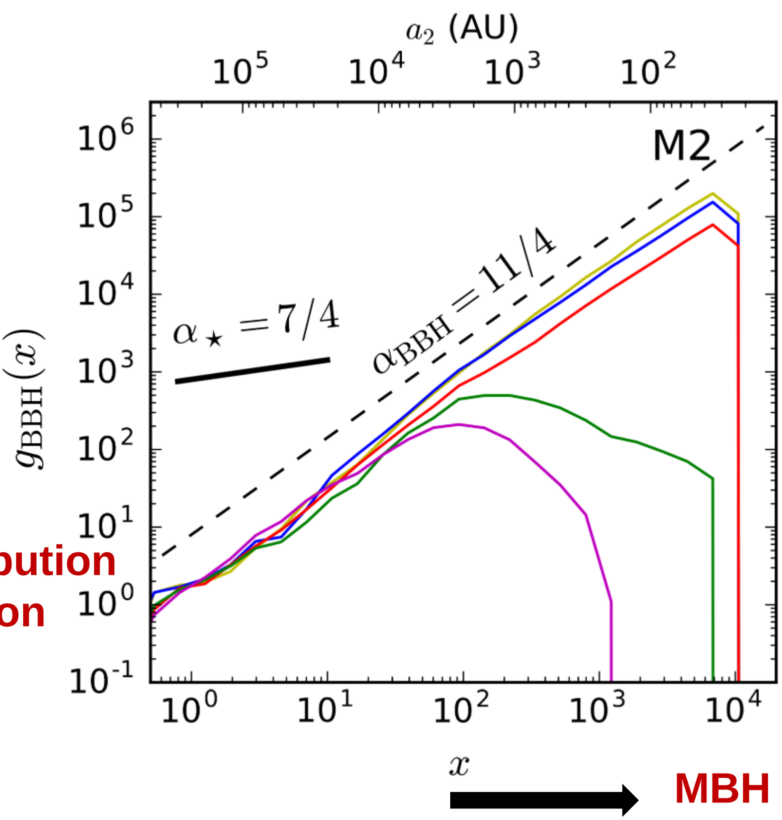

MBH

Distribution of the eccentricity in LIGO band

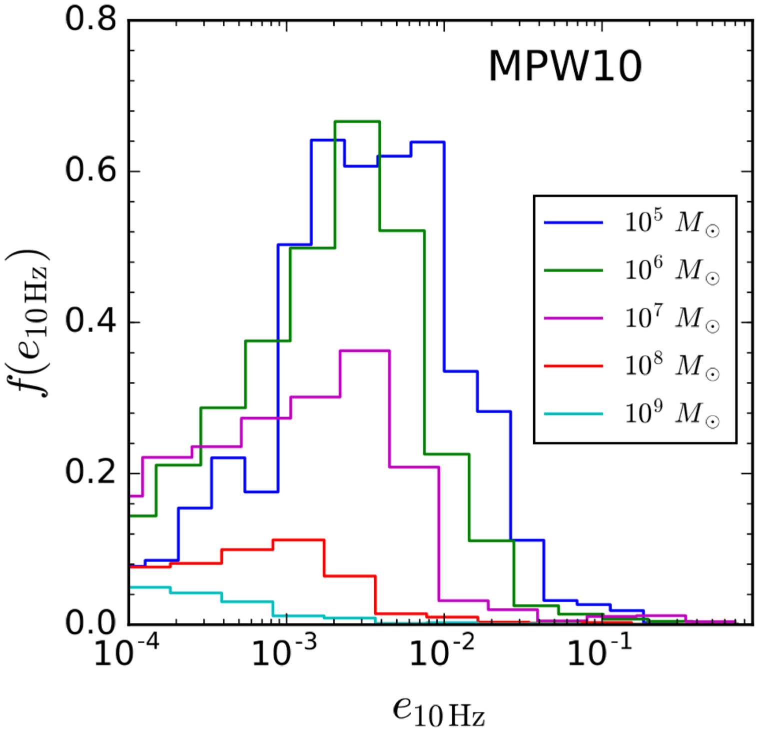

#25

Degeneracies we may encounter when testing GR using extreme-mass-ratio inspiral (EMRI)

Equatorial EMRI

KRZ EMRI system :			Kerr EMRI system :	
Deformation parameter	δ_i	Setting $\delta_i = 0$ →	Deformation parameter	δ_i=0
Source parameters	M, a, e, p,	Tuning M, a	Source parameters	M’, a’, e, p,
orbital frequencies	ω_r, ω_θ		orbital frequencies	ω_r, ω_θ

Inclined EMRI

KRZ EMRI system :			Kerr EMRI system :	
Deformation parameter	δ_i	Setting $\delta_i = 0$ →	Deformation parameter	δ_i=0
Source parameters	M, a, e, p, ι	Tuning M, a, p	Source parameters	M’, a’, e, p’, ι
orbital frequencies	$\omega_r, \omega_\theta, \omega_\phi$		orbital frequencies	$\omega_r, \omega_\theta, \omega_\phi$

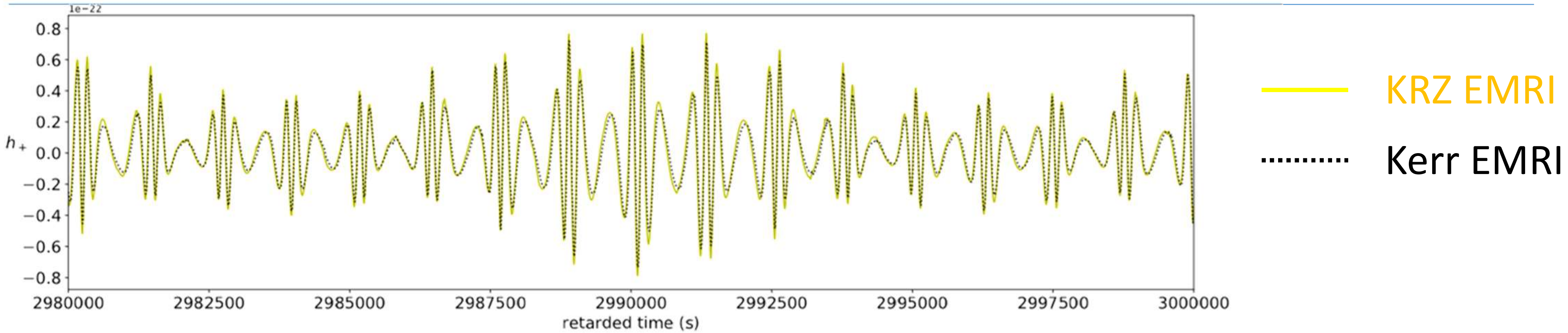

Range of parameters where degeneracy exists

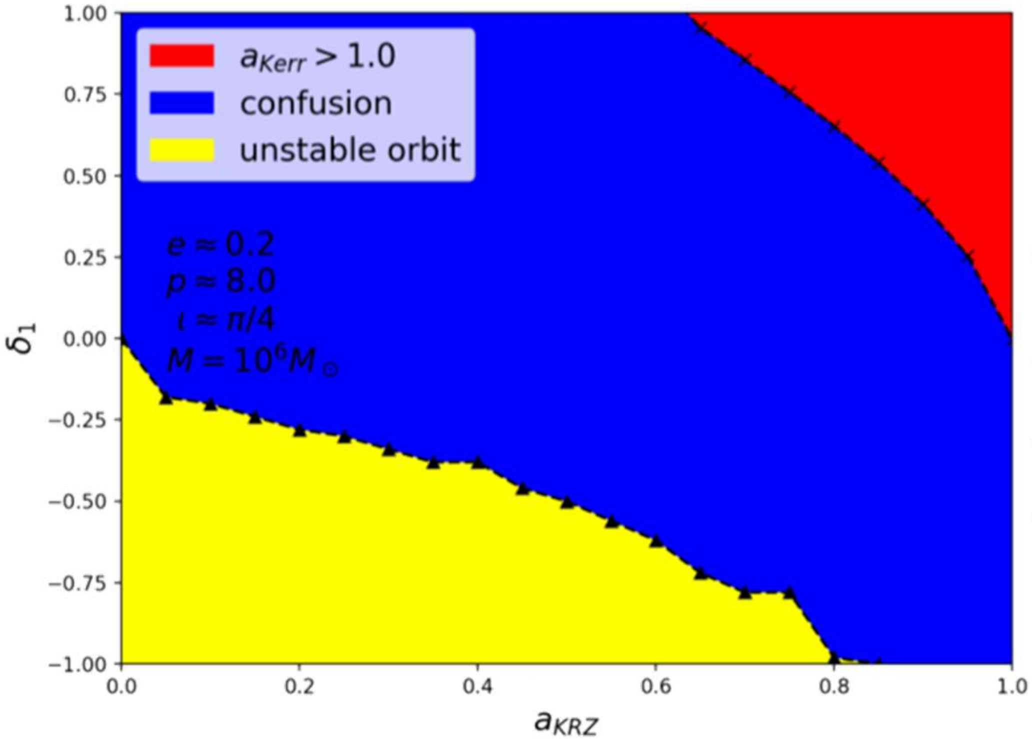

The range covers most places where $\delta_i = 0$, making test of Kerr metric impossible

Degeneracy can be broken by radiation reaction

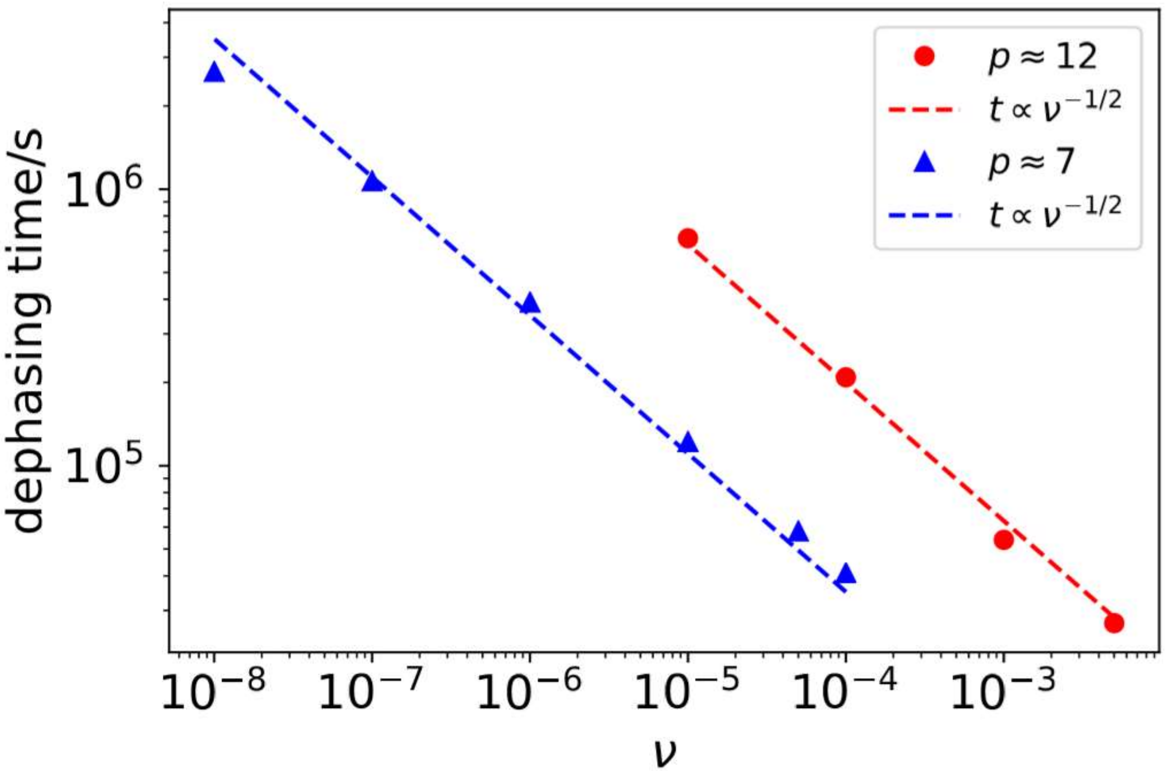

For extremely low mass-ratio ($\nu < 10^{-9}$), the time required to break the degeneracy may be up to years

#26

A *NICER* VIEW OF PSR J0030+0451:
implications for the dense matter equation of state

Geert Raaijmakers
University of Amsterdam

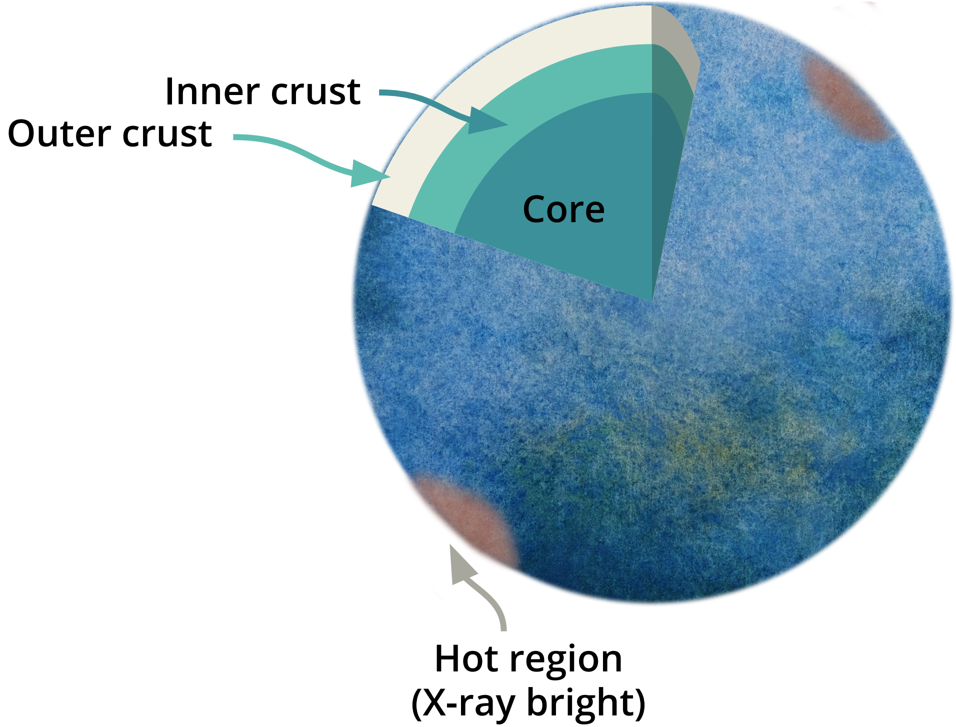

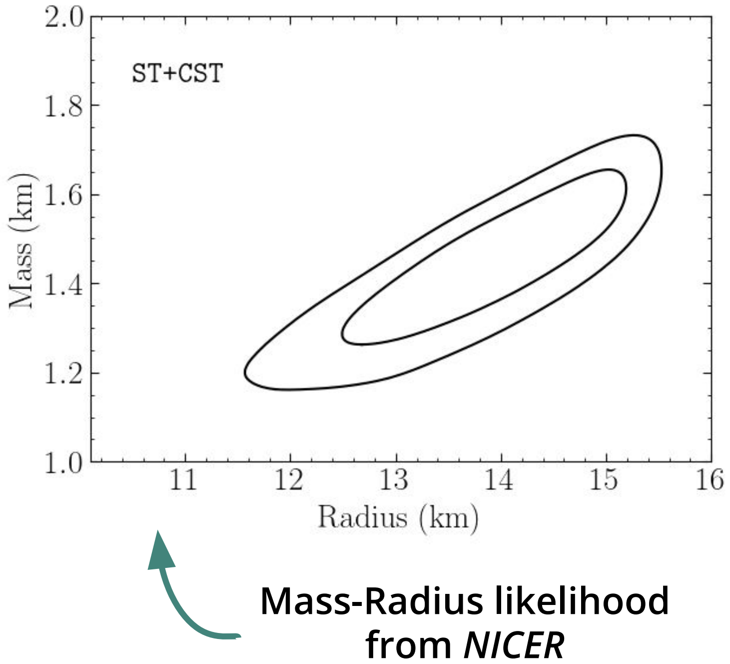

A *NICER* VIEW OF PSR J0030+0451:
implications for the dense matter equation of state

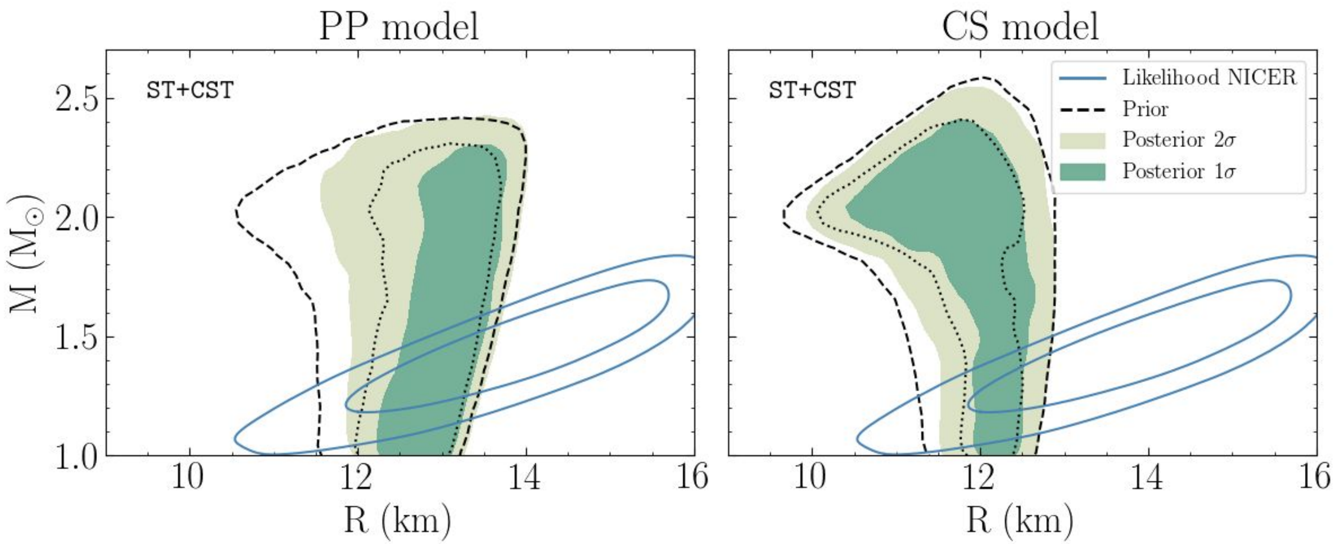

Posteriors for two EOS parameterizations